

# Persistence Exponents and the Statistics of Crossings and Occupation Times for Gaussian Stationary Processes

G. M. C. A. Ehrhardt<sup>1</sup>, Satya N. Majumdar<sup>2</sup>, and Alan J. Bray<sup>1</sup>

<sup>1</sup>*Department of Physics and Astronomy, University of Manchester, Manchester M13 9PL*

<sup>2</sup>*Laboratoire de Physique Quantique (UMR C5626 du CNRS), Université Paul Sabatier, 31062 Toulouse Cedex, France*

PACS numbers: 05.70.Ln, 05.40.+j, 02.50.-r, 81.10.Aj

We consider the persistence probability, the occupation-time distribution and the distribution of the number of zero crossings for discrete or (equivalently) discretely sampled Gaussian Stationary Processes (GSPs) of zero mean. We first consider the Ornstein-Uhlenbeck process, finding expressions for the mean and variance of the number of crossings and the ‘partial survival’ probability. We then elaborate on the correlator expansion developed in an earlier paper (G. C. M. A. Ehrhardt and A. J. Bray, Phys. Rev. Lett. 88, 070602 (2001)) to calculate discretely sampled persistence exponents of GSPs of known correlator by means of a series expansion in the correlator. We apply this method to the processes  $d^n x/dt^n = \eta(t)$  with  $n \geq 3$ , incorporating an extrapolation of the series to the limit of continuous sampling. We then extend the correlator method to calculate the occupation-time and crossing-number distributions, as well as their partial-survival distributions and the means and variances of the occupation time and number of crossings. We apply these general methods to the  $d^n x/dt^n = \eta(t)$  processes for  $n = 1$  (random walk),  $n = 2$  (random acceleration) and larger  $n$ , and to simple diffusion from random initial conditions in 1-3 dimensions. The results for discrete sampling are extrapolated to the continuum limit where possible.

## I. INTRODUCTION

Stochastic processes driven by Gaussian white noise have a wide range of applications in the physical sciences and beyond, ranging from Brownian motion to options pricing. Here we focus on two basic properties of a stochastic Gaussian time series: the number of crossings of the mean value of the series, and the fraction of time for which the series is above its mean value. The former, termed the crossing number, has long been of interest to engineers and mathematicians [1–3], and more recently to physicists [4,5]. The latter, termed the occupation time, has also been studied by mathematicians for a long time [6–8] for both Gaussian and non-Gaussian stochastic processes and has recently seen a revival in the physics community in the context of nonequilibrium systems [9–13]. The occupation-time distribution for a stochastic process is also important due to its potential applications in a variety of physical systems which include optical imaging [14], analysis of the morphology of growing surfaces [15], analysis of temperature fluctuations in weather records [16], in disordered systems [17] and also due to the connection between the occupation time in certain discrete sequences and spin-glass models [18].

Of particular interest is a limiting case of these two properties, namely the probability, termed the persistence probability [19], that the time series is always above its mean value up to time  $T$ . The latter, for stationary Gaussian time series, typically decays as  $\exp(-\theta T)$  for  $T$  large, with the exponent  $\theta$  in general taking a nontrivial value. For continuous processes  $X(T)$ , the Independent Interval Approximation (IIA) [20,21] may be used to calculate approximately (for continuous sampling) the asymptotic (i.e. large- $T$ ) forms of some of the probability distributions above. This approach, which makes the (generally invalid) assumption that the time intervals between zero-crossings are statistically independent, is surprisingly accurate in many cases. However, the IIA involves an uncontrolled approximation, which cannot be improved upon in general, and whose numerical accuracy is hard to estimate. Until now, the IIA has been the only general analytical technique available. In the absence of exact general results, calculations of probability distributions exist only for certain specific processes, although a short-time expansion for a general process has been developed [22].

Both continuous and intrinsically discrete time-series can be studied. In this paper we consider discrete-time sampling of an underlying continuous Gaussian stationary process (GSP),  $X(T)$ , with zero mean, unit variance, and known correlator  $C(T) = \langle X(T)X(0) \rangle$ . We sample this process every time step  $\Delta T$ , and study the discrete-time series  $X(i\Delta T)$ . This is, of course, completely equivalent to studying a discrete process with the same correlators  $C(j\Delta T)$ . In [23,24] we have studied the persistence of a discretely sampled random walk and of a randomly accelerated particle, both of which can be mapped to a GSP by a change of variables. In [25] we calculated, using a series expansion in the correlator  $C(j\Delta T)$ , the persistence probability for an arbitrary discretely-sampled GSP. By extrapolating to the limit in which the time between samplings tends to zero, we obtained results for several continuum processes. Thus the

results developed for discretely sampled processes may, for sufficiently smooth processes, be extended to give results for continuous-time processes.

Before going further, we illustrate the main ideas by considering the simple example of a stochastic process, the continuous-time random walk described by the Langevin equation

$$\dot{x} = \xi(t) \quad (1)$$

where  $\xi(t)$  is Gaussian white noise,  $\langle \xi(t) \rangle = 0$ , and  $\langle \xi(t)\xi(t') \rangle = 2D\delta(t-t')$ . The probability that  $x > 0$  up to time  $t$  decays as  $t^{-\theta}$  where the ‘persistence exponent’ is  $\theta = 1/2$ . This process is not stationary since its correlator,

$$C(t_1, t_2) = \langle (x(t_1) - \langle x \rangle)(x(t_2) - \langle x \rangle) \rangle = 2D \min(t_1, t_2) \quad (2)$$

does not depend only on the time difference,  $|t_1 - t_2|$ . Note that, since the process is Gaussian, it is completely specified by its correlator and mean. We can map the random walk onto a stationary process by a change of variables; we change to logarithmic time,  $T = \ln t$ , and to a normalized process  $X(T)$  via

$$X(T) \equiv \frac{x(t) - \langle x(t) \rangle}{\sqrt{\langle x(t)^2 \rangle - \langle x(t) \rangle^2}}, \quad (3)$$

obtaining the equation

$$\frac{dX}{dT} = -\frac{1}{2}X + \eta(T), \quad (4)$$

where  $\eta(T)$  is again a Gaussian white noise, and  $X(T)$  has zero mean. The process  $X(T)$  is the Ornstein-Uhlenbeck process. It is stationary, with correlator

$$C(T_1, T_2) = \langle X(T_1)X(T_2) \rangle = \exp(-|T_1 - T_2|/2). \quad (5)$$

An equivalent mapping can be made for any non-stationary Gaussian processes for which the correlator has the form  $C(t_1, t_2) = t_1^\alpha g(t_1/t_2)$ . Thus although here we only attempt to analyze stationary processes, the results are more widely applicable. Note that the exponential decay,  $\exp(-\theta T)$ , is equivalent to the power-law decay,  $t^{-\theta}$ , hence the terminology ‘persistence exponent’ for  $\theta$ .

The occupation time is the number  $s$  of positive (say) values obtained from the  $n$  measurements of  $X(T)$ . Let  $R_{n,s}$  be the probability distribution of  $s$  for given  $n$  and  $r = s/n$  be the *fraction* of measurements that are positive. In the limit  $n \rightarrow \infty$ ,  $s \rightarrow \infty$ , with  $r = s/n$  fixed,  $R_{n,s}$  has the asymptotic form  $R_{n,s} \sim [\rho(r)]^n = \exp[-\theta_D(r)T]$ , where  $T = n\Delta T$  and  $\theta_D(r) = -\ln[\rho(r)]/\Delta T$ . Here  $\theta_D(1) = \theta_D(0)$  (all or none of the measurements positive) is the usual discrete persistence exponent introduced in [23]. In a similar way we can define  $P_{n,m}$  to be the probability of observing  $m$  zero-crossings in  $n$  measurements. If now  $r = m/n$  and we take the limit  $n \rightarrow \infty$ ,  $m \rightarrow \infty$ , holding  $r =$  fixed, we find  $P_{n,m} \sim [\rho(r)]^n = \exp[-\theta_D(r)T]$ . Here  $\theta_D(0)$  (no crossings) corresponds to the usual discrete persistence. Although we use the same symbols  $\rho(r)$  and  $\theta_D(r)$  for the occupation-time and crossing problems, it should be clear from the context which problem we are referring to.

In this paper we extend the technique of [25] to calculate the exponents  $\theta_D(r)$ , or equivalently the functions  $\rho(r)$ , for the occupation-time distribution and the distribution of crossings for arbitrary discrete or discretely-sampled Gaussian stationary processes. The technique gives the exponents as a series expansion in the correlators  $C(j\Delta T)$  up to  $C(10\Delta T)$  and  $C(\Delta T)^{10}$ , i.e. 10th order. For the calculation of the persistence exponent we work to 14th order. The results work well for  $C(j\Delta T)$  small, i.e. the time between samplings large compared to the correlation time of the stationary process. For certain processes we are able to extrapolate the series to the limit  $\Delta T \rightarrow 0$ , thus obtaining values of the continuum exponents that compare favourably with those predicted by the IIA when measured against exact or numerical results.

The layout of this paper is as follows: In Part I we consider the Ornstein-Uhlenbeck process introduced above, this being perhaps the simplest of GSPs. By extending the ‘matrix method’ developed in [23] we find the mean and variance of the distribution of zero-crossings as a perturbation expansion to high accuracy. We also use another method to find the same results. The case of an unstable potential (obtained by changing the sign of the drift term) is also considered. We extend the concept of partial survival [4] to discrete sampling, calculating  $F_n(p)$ , the probability of surviving to  $n$  samplings if each detected zero-crossing is survived with probability  $p$ .

In Part II we apply and extend the correlator expansion method of calculating the persistence exponents, occupation-time distribution and crossing distribution of an arbitrary discretely-sampled GSP. The general method is then applied to some specific examples of interest, and the results extrapolated to the limit of continuum sampling where possible.

In section VI we introduce the correlator expansion first developed to 14th order in [25] as a method of calculating discretely-sampled persistence exponents. We explain this technique more fully including the extrapolation to the continuum limit using constrained Padé approximants, which allows rather accurate calculation of the standard persistence exponents. In [25] this technique was applied to the case of the random acceleration process and also to diffusion from random initial conditions in 1-3 dimensions. Here we also apply it to the class of processes  $d^n x/dt^n = \eta(t)$  where  $\eta(t)$  is Gaussian white noise. The  $n = 1, 2$  cases are the random walk and random acceleration problems already studied. Here we calculate the persistence exponents for larger values of  $n$  and show numerically that  $\theta_n - \theta_\infty \propto 1/n$  for  $n$  large. The results are compared to the predictions of the Independent Interval Approximation (IIA).

In Sections VII and VIII we extend the correlator expansion to calculate the occupation-time distribution,  $R_{n,s}$ , this being the probability of  $s$  positive measurements in  $n$  samplings, to 10th order in the correlator. This gives, in particular, the variance of the occupation-time distribution which we calculate in a more straightforward way as a check. We define a partial-survival occupation probability,  $P_n(p)$ , as the probability of surviving to  $n$  samplings if each positive sampling is survived with probability  $p$ . This is also the generating function for  $R_{n,s}$ . We find  $P_n(p)$  to 14th order in the correlator. We apply the results to the following five GSPs: the random walk, where the results of Part I are used as a check of the method, the random acceleration problem and diffusion from random initial conditions in 1, 2 and 3 dimensions. Extrapolations to the continuum are included.

In Sections IX, X and XI we further extend the correlator expansion to calculate  $P_{n,m}$ , the probability of  $m$  detected crossings in  $n$  samplings. This is found to 10th order in the correlator and also enables us to calculate the partial-survival probability and the moments of the crossing distribution. We apply the result to the five GSPs of section VII, and also to the  $d^n x/dt^n = \eta(t)$  processes for  $n > 2$  and to an intrinsically discrete process for which the exact results are known [5]. Extrapolations to the continuum are included and we compare continuum results with the IIA and also, for the random acceleration partial-survival problem and the intrinsically discrete process, to the exact solutions. In Section X we show the result for the mean number of detected crossings. We also derive the variance as a series expansion in the correlator, the coefficients of which agree with those of the previous section. We conclude with brief summary of the results.

## Part I

# The Ornstein-Uhlenbeck Process

In Part I we will study the detected crossings of the Ornstein-Uhlenbeck process. Beside being of interest in its own right, this will illustrate some of the methods used later and also provide several checks on the correlator expansion of Part II. Furthermore, here we are able to calculate probability distributions starting at a certain position  $X_0$ , rather than just the long-time or stationary state distributions.

Consider the stationary Gaussian Markov process evolving via the Langevin equation,

$$\frac{dX}{dT} = -\mu X + \eta(T), \quad (6)$$

where  $\eta(T)$  is a white noise with mean zero and correlator,  $\langle \eta(T)\eta(T') \rangle = 2D\delta(T-T')$ . This is the Ornstein-Uhlenbeck process whose persistence exponent for discrete sampling was calculated in [23].

Integrating equation (6), we get

$$X(T) = X_0 e^{-\mu T} + e^{-\mu T} \int_0^T \eta(T_1) e^{\mu T_1} dT_1, \quad (7)$$

where  $X_0 = X(T=0)$ . Let  $T = n\Delta T$ . Then the mean position  $\langle X_n \rangle$  after  $n$  steps starting initially at  $X_0$  is given from equation (7) by,

$$\langle X_n \rangle = X_0 e^{-\mu n \Delta T} = X_0 a^n, \quad (8)$$

where  $a = e^{-\mu \Delta T}$ . Similarly one finds that the correlation function is given by,

$$\langle [X_n - \langle X_n \rangle][X_m - \langle X_m \rangle] \rangle = D'(a^{|n-m|} - a^{n+m}), \quad (9)$$

where  $D' = D/\mu$ . Thus in the stationary state,  $n \rightarrow \infty$ ,  $m \rightarrow \infty$  with  $n - m$  fixed, this process has mean zero and a correlator  $C(T_1, T_2) \equiv \langle X(T_1)X(T_2) \rangle$  given by

$$C(T_1, T_2) = C(|T_2 - T_1|) = D' e^{-\mu|T_2 - T_1|}. \quad (10)$$

## II. DISCRETE BACKWARD FOKKER-PLANCK EQUATION

Let  $Q_n(m, X)$  be the probability that starting at  $X$  at  $T = 0$ , the process, *when sampled only at the discrete points*, changes sign  $m$  times within  $n$  discrete steps. Note that the probability  $P_{n,m}$  of observing  $m$  sign changes in  $n$  measurements (as defined in the introduction) can be simply obtained from  $Q_n(m, X)$  via the relation,  $P_{n,m} = \int_{-\infty}^{\infty} Q_n(m, X) p_0(X) dX$  where  $p_0(X)$  is the initial distribution of  $X$  which we will take as the stationary distribution of  $X$ . One can write down a recursion relation for  $Q_n(m, X)$ , valid for  $X > 0$ , by noting that at the first step either the process changes sign or it does not.

$$Q_{n+1}(m, X) = \int_0^{\infty} Q_n(m, Y) G(Y, \Delta T | X, 0) dY + \int_{-\infty}^0 Q_n(m-1, Y) G(Y, \Delta T | X, 0) dY, \quad (11)$$

where  $G(Y, \Delta T | X, 0)$  is the probability of going from  $X$  to  $Y$  in a time  $\Delta T$ , given by

$$G(Y, \Delta T | X, 0) = \frac{1}{\sqrt{2\pi D'(1-a^2)}} e^{-\frac{(Y-aX)^2}{2D'(1-a^2)}}. \quad (12)$$

Using the rescaled variables  $x = X/\sqrt{D'(1-a^2)}$  and  $y = Y/\sqrt{D'(1-a^2)}$ , and making use of the symmetry  $Q_n(m, -x) = Q_n(m, x)$  we get,

$$Q_{n+1}(m, x) = \frac{1}{\sqrt{2\pi}} \int_0^{\infty} \left[ Q_n(m, y) e^{-(y-ax)^2/2} + Q_n(m-1, y) e^{-(y+ax)^2/2} \right] dy. \quad (13)$$

Note that for  $m = 0$  this reduces to the persistence problem studied in [23], whilst for  $m = n$  we have the ‘alternating persistence’ problem [23].

We define the generating function,  $F_n(p, x) = \sum_{m=0}^n Q_n(m, x) p^m$ . The generating function has a physical interpretation: If one considers that with every detected change of sign a particle survives with probability  $p$  (partial survival), then  $F_n(p, x)$  is precisely the survival probability of the particle. Note that for  $p = 1$  this probability is 1 whilst for  $p = 0$  we recover the usual discrete persistence.

Multiplying equation (13) by  $p^m$  and summing over  $m$  we get,

$$F_{n+1}(p, x) = \frac{1}{\sqrt{2\pi}} \int_0^{\infty} F_n(p, y) \left[ e^{-(y-ax)^2/2} + p e^{-(y+ax)^2/2} \right] dy. \quad (14)$$

Let  $E_n(x) = \sum_{m=0}^{\infty} m Q_n(m, x) = dF_n(p, x)/dp|_{p=1}$  denote the expected number of sign changes up to  $n$  steps starting at  $x$  at  $T = 0$ . Taking the derivative with respect to  $p$  and putting  $p = 1$  in equation (14), it follows that  $E_n(x)$  satisfies the recursion relation,

$$E_{n+1}(x) = \frac{1}{\sqrt{2\pi}} \int_0^{\infty} E_n(y) \left[ e^{-(y-ax)^2/2} + e^{-(y+ax)^2/2} \right] dy + \frac{1}{2} \operatorname{erfc} \left( \frac{ax}{\sqrt{2}} \right), \quad (15)$$

where  $\operatorname{erfc}(x)$  is the standard complimentary error function and the recursion in equation (15) starts with the initial condition,  $E_0(x) = 0$ . Also note that  $G_n(x) = \sum_{m=0}^{\infty} m(m-1) Q_n(m, x) = d^2 F_n(p, x)/dp^2|_{p=1}$  satisfies the recursion,

$$G_{n+1}(x) = \frac{1}{\sqrt{2\pi}} \int_0^{\infty} G_n(y) \left[ e^{-(y-ax)^2/2} + e^{-(y+ax)^2/2} \right] dy + \frac{2}{\sqrt{2\pi}} \int_0^{\infty} dy E_n(y) e^{-(y+ax)^2/2}, \quad (16)$$

with the initial condition  $G_0(x) = 0$ , and where  $E_n(x)$  is given by the solution of equation (15). In order to calculate the average number of crossings and the variance around this average, we need to solve the two integral equations (15) and (16).

If we can obtain the solution of  $E_n(x)$  from equation (15), then we need to average over the distribution of the initial position  $x$  to obtain  $\langle m \rangle_n = \int_{-\infty}^{\infty} E_n(x) p_0(X) dX$  where  $p_0(X)$  is the initial distribution of the position  $X$  and  $x = X/\sqrt{D'(1-a^2)}$ . For  $a < 1$ , i.e.  $\mu > 0$ , if we choose  $p_0(X)$  to be the stationary distribution of the process,  $p_0(X) = \frac{1}{\sqrt{2\pi D'}} e^{-X^2/2D'}$ , which corresponds to waiting an infinitely large number of steps before starting the measurements, then  $\langle m \rangle_n$  can be computed exactly from equation (15). Multiplying equation (15) by this  $p_0(X)$  and integrating over  $X$  we get

$$\langle m \rangle_{n+1} = \langle m \rangle_n + \lambda, \quad (17)$$

where  $\lambda = \frac{1}{2} - \frac{1}{\pi} \sin^{-1}(a)$ . Using  $\langle m \rangle_0 = 0$ , we get exactly,

$$\langle m \rangle_n = n\lambda \quad (18)$$

which is the random walk case of the general result  $\langle m \rangle_n/n = 1/2 - (1/\pi) \sin^{-1} C(\Delta T)$  [26]. Note that for  $\Delta T \rightarrow 0$  this reduces to Rice's formula, while for  $\Delta T \rightarrow \infty$  it reduces to  $n/2$  as expected since the values of  $X$  at the discrete points become statistically independent. Note that for  $a > 1$ , there is no stationary distribution as this corresponds to an unstable potential.

Note however that to compute  $g_n = \langle m(m-1) \rangle_n$  by a similar method, we need to know the full function  $E_n(x)$ , that is we need to solve the full integral equation (15). Indeed for  $a < 1$ , if we choose to average over the stationary distribution,  $p_0(X) = \frac{1}{\sqrt{2\pi D'}} e^{-X^2/2D'}$ , then by multiplying both sides of equation (16) by  $p_0(X)$  and integrating over  $x$  from  $-\infty$  to  $\infty$ , we get after straightforward algebra

$$g_{n+1} = g_n + \sqrt{\frac{2(1-a^2)}{\pi}} \int_0^\infty E_n(y) e^{-D'(1-a^2)y^2/2} \operatorname{erfc}\left(\frac{ay}{\sqrt{2}}\right) dy. \quad (19)$$

Hence the variance of the number of crossings,  $\sigma_n^2 = \langle m^2 \rangle_n - \langle m \rangle_n^2$  is given by,

$$\sigma_n^2 = g_n + n\lambda - n^2\lambda^2, \quad (20)$$

where  $g_n$  is given by the solution of the recursion equation (19) and  $\lambda = \frac{1}{2} - \frac{1}{\pi} \sin^{-1}(a)$ . To determine  $g_n$  from equation (19), we need to know the full function  $E_n(x)$ .

In the next section, we show that there is an alternative way to derive an expression for  $E_n(x)$  without solving the integral equation (15).

### III. ALTERNATIVE DERIVATION OF $E_{\mathbf{N}}(X)$

An alternative derivation of  $E_n(X)$  can be obtained by noting the evident relation,

$$\begin{aligned} E_{n+1}(X) - E_n(X) &= \frac{1}{2} [1 - \langle \operatorname{sign}(X_n) \operatorname{sign}(X_{n+1}) \rangle] \\ &= \langle \theta(X_n) \rangle + \langle \theta(X_{n+1}) \rangle - 2\langle \theta(X_n) \theta(X_{n+1}) \rangle, \end{aligned} \quad (21)$$

where  $\theta(x)$  is the standard theta function. Noting that  $X_n$  and  $X_{n+1}$  are Gaussian variables, we can compute the right hand side of equation (21) exactly. For this we first need the joint distribution  $P[X_n, X_{n+1}]$  of  $X_n$  and  $X_{n+1}$  which involves the correlation matrix  $C_{n,n+1}$  given by

$$C_{n,n+1} = D' \begin{bmatrix} 1 - a^{2n} & a(1 - a^{2n}) \\ a(1 - a^{2n}) & 1 - a^{2n+2} \end{bmatrix}$$

where we have used equation (9) for the matrix elements. Using this joint distribution and carrying out the Gaussian integrations, we get after lengthy but straightforward algebra the final expression of the right hand side of equation (21) as,

$$\begin{aligned} E_{n+1}(X) - E_n(X) &= \frac{1}{2} \operatorname{erfc}(-A_n X) + \frac{1}{2} \operatorname{erfc}(-A_{n+1} X) \\ &\quad - \frac{1}{\sqrt{\pi}} \int_{-A_{n+1} X}^\infty dy e^{-y^2} \operatorname{erfc} \left[ -\sqrt{\frac{1-a^{2n+2}}{1-a^2}} A_n X - a \sqrt{\frac{1-a^{2n}}{1-a^2}} y \right], \end{aligned} \quad (22)$$

where  $A_n = a^n / \sqrt{2D'(1-a^{2n})}$ . Changing to rescaled variable,  $x = X / \sqrt{D'(1-a^2)}$  and using the initial condition  $E_0(x) = 0$ , we get from equation (22),

$$\begin{aligned} E_n(x) &= \frac{1}{2} \sum_{m=0}^{n-1} \left[ \operatorname{erfc} \left( -\frac{a^m x}{\sqrt{2}} \sqrt{\frac{1-a^2}{1-a^{2m}}} \right) + \operatorname{erfc} \left( -\frac{a^{m+1} x}{\sqrt{2}} \sqrt{\frac{1-a^2}{1-a^{2m+2}}} \right) \right. \\ &\quad \left. - \frac{2}{\sqrt{\pi}} \int_{-\frac{a^{m+1} x}{\sqrt{2}} \sqrt{\frac{1-a^2}{1-a^{2m+2}}}}^\infty dy e^{-y^2} \operatorname{erfc} \left( -\sqrt{\frac{1-a^{2m+2}}{1-a^2}} \sqrt{\frac{1-a^2}{1-a^{2m}}} \frac{a^m}{\sqrt{2}} x - a \sqrt{\frac{1-a^{2m}}{1-a^2}} y \right) \right]. \end{aligned} \quad (23)$$

This can be solved numerically, figure (1) shows  $E_n(x) - n\lambda$  for  $a = 1/2$  and  $n = 1000$ .

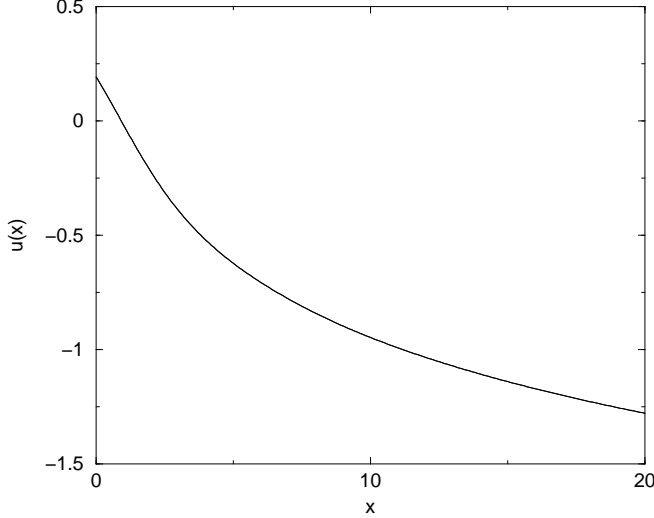


FIG. 1. Plot of  $u(x) = E_n(x) - n\lambda$  for  $a = 1/2$  and  $n = 1000$ , calculated using equation (23).  $u(x)$  is symmetric about  $x = 0$ . Also shown is  $u(x)$  for  $a = 1/2$  derived using the matrix method (equation(30)), the two curves are indistinguishable.

In the next section we discuss the exact asymptotic properties of the mean and the variance of the number of sign changes for the two cases: (A) Stable potential,  $\mu > 0$ , i.e  $0 < a < 1$  and (B) unstable potential,  $\mu < 0$ , i.e.  $a > 1$ .

#### IV. ASYMPTOTICS OF THE MEAN AND VARIANCE OF THE NUMBER OF SIGN CHANGES

##### A. Stable potential: $\mu > 0$

In this case  $a = e^{-\mu\Delta T} < 1$  and also  $D' > 0$ . Thus as  $n \rightarrow \infty$ ,  $A_n = a^n / \sqrt{2D'(1-a^2)} \rightarrow 0$ . Then from equation (22), we find  $E_{n+1}(X) - E_n(X) \rightarrow \lambda$  with  $\lambda = \frac{1}{2} - \frac{1}{\pi} \sin^{-1}(a)$  indicating that in the  $n \rightarrow \infty$  limit,  $E_n(X)$  becomes independent of  $X$  (as long as  $X < a^n$ ) and to leading order for large  $n$ ,

$$E_n(x) = n\lambda, \quad (24)$$

in agreement with equation (18). Indeed the expression for  $E_n(x)$  in equation (23) is a solution of the integral equation (15). For finite  $n$ , one can write  $E_n(x) = n\lambda + u_n(x)$ . An explicit expression for  $u_n(x)$  can be obtained from that of  $E_n(x)$  in equation (23). Using the explicit value of  $\lambda$  and after a few steps of algebra we get,

$$\begin{aligned} u_n(x) &= \frac{1}{2} \sum_{m=0}^{n-1} s_m(x) \\ s_m(x) &= \operatorname{erfc} \left( -\frac{a^m x}{\sqrt{2}} \sqrt{\frac{1-a^2}{1-a^{2m}}} \right) + \operatorname{erfc} \left( -\frac{a^{m+1} x}{\sqrt{2}} \sqrt{\frac{1-a^2}{1-a^{2m+2}}} \right) - 2 + \frac{2}{\sqrt{\pi}} \int_0^\infty dy e^{-y^2} \operatorname{erfc} \left( \frac{-ay}{\sqrt{1-a^2}} \right) \\ &\quad - \frac{2}{\sqrt{\pi}} \int_{-\frac{xa^{m+1}}{\sqrt{2}} \sqrt{\frac{1-a^{2m}}{1-a^{2m+2}}}}^\infty dy e^{-y^2} \operatorname{erfc} \left( -\sqrt{\frac{1-a^{2m+2}}{1-a^2}} \sqrt{\frac{1-a^2}{1-a^{2m}}} \frac{a^m}{\sqrt{2}} x - a \sqrt{\frac{1-a^{2m}}{1-a^2}} y \right). \end{aligned} \quad (25)$$

Besides, using  $E_n(x) = n\lambda + u_n(x)$  in the integral equation (15), we find that  $u_n(x)$  also satisfies the following integral equation,

$$u_{n+1}(x) = \frac{1}{\sqrt{2\pi}} \int_0^\infty u_n(y) \left[ e^{-(y-ax)^2/2} + e^{-(y+ax)^2/2} \right] dy + \frac{1}{2} \operatorname{erfc} \left( \frac{ax}{\sqrt{2}} \right) - \lambda, \quad (26)$$

with  $\lambda = \frac{1}{2} - \frac{1}{\pi} \sin^{-1}(a)$ .

Now the leading term in  $E_n(x)$  is  $n\lambda$  and is independent of  $x$  as long as  $x < a^{-n}$ . This upper cut-off tends to  $\infty$  as  $n \rightarrow \infty$  since  $a < 1$ . The  $x$  dependence of  $E_n(x)$  appears only in the subleading term  $u_n(x)$ . Now, as  $n \rightarrow \infty$ ,  $u_n(x)$  tends to a stationary solution independent of  $n$  (as long as  $x \ll a^{-n}$ ) and is given by the fixed point solution  $u(x)$  of the integral equation (26),

$$u(x) = \frac{1}{\sqrt{2\pi}} \int_0^\infty u(y) \left[ e^{-(y-ax)^2/2} + e^{-(y+ax)^2/2} \right] dy + \frac{1}{2} \operatorname{erfc} \left( \frac{ax}{\sqrt{2}} \right) - \lambda. \quad (27)$$

We can find  $u_n(x)$  perturbatively by expanding the  $axy$  term in the exponentials in equation (27) to get,

$$u(x) = \frac{1}{\sqrt{2\pi}} \sum_{m=0}^{\infty} \sum_{(\text{meven})} \frac{(ax)^m e^{-(ax)^2/2}}{m!} \int_0^\infty u(y) e^{-y^2/2} 2y^m dy + \frac{1}{2} \operatorname{erfc} \left( \frac{ax}{\sqrt{2}} \right) - \lambda. \quad (28)$$

Defining

$$I_l = \int_0^\infty u(x) \frac{a^{l/2} x^l}{\sqrt{l!}} e^{-x^2/2} dx \quad (29)$$

gives

$$u(x) = \sqrt{\frac{2}{\pi}} \sum_{m=0}^{\infty} \sum_{(\text{meven})} \frac{a^{m/2} x^m e^{-(ax)^2/2}}{\sqrt{m!}} I_m + \frac{1}{2} \operatorname{erfc} \left( \frac{ax}{\sqrt{2}} \right) - \lambda. \quad (30)$$

Multiplying both sides by  $a^{l/2} x^l e^{-x^2/2} / \sqrt{l!}$  and integrating over positive  $x$  gives,

$$I_l = \sum_{m=0}^{\infty} \sum_{(\text{meven})} M_{lm} I_m + J_l \quad (31)$$

where

$$M_{lm} = \frac{1}{\sqrt{2\pi a}} \left( \frac{2a}{1+a^2} \right)^{(l+m+1)/2} \frac{\Gamma[(l+m+1)/2]}{\sqrt{l!m!}} \quad \text{m even, 0 otherwise} \quad (32)$$

$$J_l = \frac{a^{l/2}}{\sqrt{l!}} \int_0^\infty x^l e^{-x^2/2} \left[ \frac{1}{2} \operatorname{erfc} \left( \frac{ax}{\sqrt{2}} \right) - \lambda \right]. \quad (33)$$

Thus

$$\mathbf{I} = (\mathbf{1} - \mathbf{M})^{-1} \mathbf{J} \quad (34)$$

This perturbative expansion in  $a$  is the matrix method. Although  $M_{lm}$  is an infinite array, the elements decrease rapidly with increasing  $l$  and  $m$  since each increment of  $l$  and  $m$  gives a higher power of  $a$  ( $a < 1$ ). We can solve this numerically. Figure 1 shows  $u(x)$  for  $a = 1/2$ . Alternatively, using MATHEMATICA, we can solve equation (31) iteratively. At each iteration we obtain a new  $\mathbf{I}$  whose elements are a series in  $a$  up to our required order. Convergence is rapid. This can only be done with a smaller matrix than the numerical method, but gives a result for general  $a$ . Note that we could equivalently have done this perturbative expansion on equation (15) to get  $E(x)$  and subtracted the  $n\lambda$ .

Alternatively, we can directly take the  $n \rightarrow \infty$  limit of the expression of  $u_n(x)$  in equation (25) to get,

$$u(x) = \frac{1}{2} \sum_{m=0}^{\infty} s_m(x), \quad (35)$$

where  $s_m(x)$  is given by equation (25). This has been done numerically (for  $n$  large but finite) and found to agree with the matrix method.

Let us first compute the asymptotic properties of the fixed point solution  $u(x)$ . Consider first the limit  $x \rightarrow 0$ . Putting  $x = 0$  in equation (25) and carrying out the integrations we get, after some algebra,

$$u(0) = \frac{1}{\pi} \sum_{m=0}^{\infty} \sin^{-1} \left[ \frac{a\sqrt{1-a^2}}{\sqrt{1-a^{2m+2}}} \left(1 - \sqrt{1-a^{2m}}\right) \right]. \quad (36)$$

For example, for  $a = 1/2$ , we get  $u(0) = 0.19160374\dots$  which agrees very well with the result obtained from the direct numerical integration of equation (26) in the large  $n$  limit. Consider now the other limit  $x \rightarrow \infty$ . By making the change of variable,  $y - ax = \sqrt{2}z$  in the integral equation (27), we get to leading order for large  $x$  (where the lower limit of the first integration  $\rightarrow -\infty$ ),

$$u(x) \approx u(ax) - \lambda. \quad (37)$$

The solution of this equation is given by,

$$u(x) \approx \frac{\lambda}{\ln a} \ln x. \quad (38)$$

Note that  $\lambda/\ln a < 0$  for  $a < 1$  and hence  $u(x)$  goes to  $-\infty$  logarithmically as  $x \rightarrow \infty$ . This is consistent with the fact that  $E_n(x) \approx n\lambda + \lambda \frac{\ln x}{\ln a} \sim \frac{\lambda}{\ln a} \ln(xa^n) \rightarrow 0$  as  $x \rightarrow a^{-n}$  as it should evidently from the direct expression of  $E_n(x)$  in equation (23).

In figure 1, we plot  $u(x)$  obtained from numerically evaluating the sum in equation (25) and also the result obtained using the matrix method. The results agree to within numerical precision. Also, they agree with the asymptotic results in the large and small  $x$  limits. Note that the  $x \rightarrow \infty$  limit was not attainable by the matrix or summation methods because in both cases the evaluation is done to a finite order or finite  $n$ .

Once we know  $u_n(x)$ , then we can determine the variance  $\sigma_n^2$  from equation (20). Substituting  $E_n(x) = n\lambda + u_n(x)$  in equation (19) and using the fact that  $u_n(x)$  tends to the fixed point solution  $u_n(x) \rightarrow u(x)$  for large  $n$ , we get

$$g_{n+1} = g_n + 2n\lambda^2 + \beta, \quad (39)$$

where

$$\beta = \sqrt{\frac{2(1-a^2)}{\pi}} \int_0^{\infty} u(y) e^{-D'(1-a^2)y^2/2} \operatorname{erfc}\left(\frac{ay}{\sqrt{2}}\right) dy. \quad (40)$$

One can easily solve the recursion equation (39) exactly using  $g_0 = 0$  and we get,

$$g_n = \lambda^2 n^2 + (\beta - \lambda^2)n, \quad (41)$$

where  $\beta$  is given by equation (40). Substituting this expression for  $g_n$  in equation (20), we finally get the required exact expression of the variance for large  $n$ ,

$$\sigma_n^2 = (\lambda - \lambda^2 + \beta) n. \quad (42)$$

Thus the variance can be exactly determined once we know the function  $u(x)$  and thereby  $\beta$  from equation (40). Using the exact expression of  $u(x)$  from equation (35), we have, in principle, an exact result for  $\beta$  and hence for  $\sigma_n^2$ . Substituting the  $u(x)$  derived from the matrix method into equation (40) gives  $\beta$  and hence  $\sigma_n^2$ .  $\sigma_n^2/n$  is plotted as a function of  $a$  for  $D' = 1$  in figure (2).

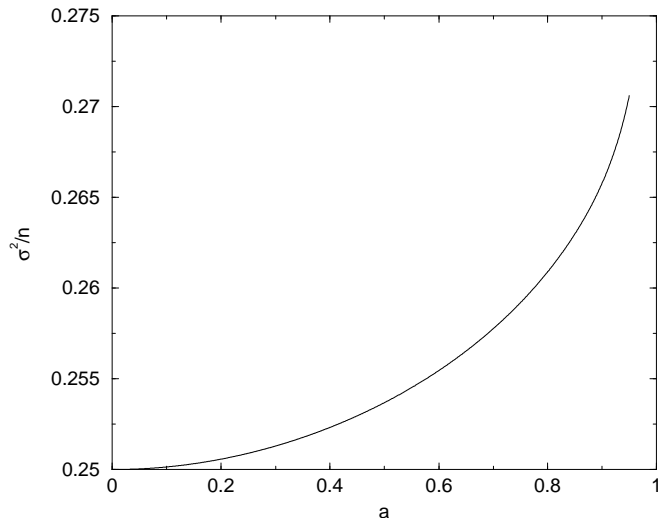




FIG. 2. Plot of  $\sigma_n^2/n$  against  $a = e^{-\mu\Delta T}$  with  $D' = 1$ . Note that  $\sigma_n^2/n \rightarrow \infty$  for  $a \rightarrow 1$ , and the series has not converged for large  $a$ .

### B. Unstable potential: $\mu < 0$

In the previous subsection, we have seen that for  $a < 1$ , the function  $E_n(x)$  behaves asymptotically for large  $n$  as  $E_n(x) = n\lambda + u(x)$  where  $u(x)$  is given either by the exact expression in equation (35) or equivalently by the solution of the integral equation (27). For the unstable potential  $\mu < 0$ , i.e.  $a > 1$ , the number of crossings will be finite and so  $E_n(x)$  approaches a steady state as  $n \rightarrow \infty$ . This is most easily seen from equation (22). For  $a > 1$ ,  $A_n = a^n / \sqrt{2D'(1-a^2)} \rightarrow \infty$  as  $n \rightarrow \infty$  (note that  $D' = D/\mu < 0$ ). Taking this limit in equation (22), we see that  $E_{n+1}(x) - E_n(x) \rightarrow 0$  for all  $x$  as  $n \rightarrow \infty$ , indicating  $E_n(x) \rightarrow E(x)$  as  $n \rightarrow \infty$ . This steady state  $E(x)$  is given by the fixed point solution of the integral equation (15) with  $a > 1$ ,

$$E(x) = \frac{1}{\sqrt{2\pi}} \int_0^\infty E(y) \left[ e^{-(y-ax)^2/2} + e^{-(y+ax)^2/2} \right] dy + \frac{1}{2} \operatorname{erfc} \left( \frac{ax}{\sqrt{2}} \right). \quad (43)$$

$E(x)$  can be found using the matrix method in the same way as before but with  $J_l$  replaced by  $J'_l$  where

$$J'_l = \frac{a^{l/2}}{\sqrt{l!}} \int_0^\infty x^l e^{-x^2/2} \frac{1}{2} \operatorname{erfc} \left( \frac{ax}{\sqrt{2}} \right). \quad (44)$$

$E(x)$  is shown in figure (3) for the case  $a = 2$ .

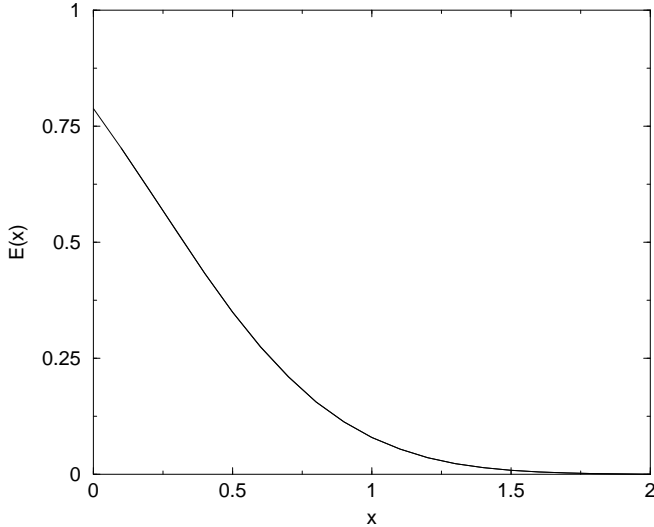


FIG. 3. The expected number of detected crossings  $E(x)$  for the case  $a = 2$  (unstable potential). Shown are the results of the matrix method and also numerical evaluation of equation (45) which are indistinguishable.

Alternatively,  $E(x)$  is also given by taking the  $n \rightarrow \infty$  limit of the exact expression in equation (23) (with  $a > 1$ ),

$$E(x) = \frac{1}{2} \sum_{m=0}^{\infty} \left[ \operatorname{erfc} \left( -\frac{a^m x}{\sqrt{2}} \sqrt{\frac{1-a^2}{1-a^{2m}}} \right) + \operatorname{erfc} \left( -\frac{a^{m+1} x}{\sqrt{2}} \sqrt{\frac{1-a^2}{1-a^{2m+2}}} \right) \right. \\ \left. - \frac{2}{\sqrt{\pi}} \int_{-\frac{a^{m+1}x}{\sqrt{2}}}^{\frac{a^m x}{\sqrt{2}}} \sqrt{\frac{1-a^{2m}}{1-a^{2m+2}}} dy e^{-y^2} \operatorname{erfc} \left( -\sqrt{\frac{1-a^{2m+2}}{1-a^2}} \sqrt{\frac{1-a^2}{1-a^{2m}}} \frac{a^m}{\sqrt{2}} x - a \sqrt{\frac{1-a^{2m}}{1-a^2}} y \right) \right]. \quad (45)$$

This is shown in figure (3).

We have calculated the variance of the number of detected crossings and also the expected number of detected crossings starting at position  $x$ . These calculations have been carried out by two independent methods and the results agree with other.

## V. PARTIAL SURVIVAL

The partial-survival probability,  $F_n(p, x)$ , is the probability of surviving beyond the  $n$ th sampling having started at  $x$  if each detected crossing of the origin is survived with probability  $p$ . Thus,

$$F_n(p, x) = \sum_{m=0}^{\infty} Q_n(m, x) p^m \quad (46)$$

and as stated before  $F_n(p, x)$  is the generating function for  $Q_n(m, x)$ .  $F_n(p, x)$  satisfies the integral equation (14). We expect that for large  $n$ ,  $F_n(p, x) = [\rho_p(a)]^n F(x)$  where  $\rho_p(a) = e^{-\theta(p)\Delta T}$  and  $\theta(p)$  is the discrete persistence exponent. Substituting this into equation (14), we get an eigenvalue equation for  $F(x)$ ,

$$\rho_p(a)F(x) = \frac{1}{\sqrt{2\pi}} \int_0^{\infty} F(y) \left[ e^{-(y-ax)^2/2} + p e^{-(y+ax)^2/2} \right] dy. \quad (47)$$

The largest eigenvalue  $\rho_p(a)$  and the corresponding eigenfunction can then be determined either by the matrix method or by the variational method as in our previous paper [23]. Using the matrix method, we get,

$$\rho_p(a)F(x) = \frac{e^{-a^2 x^2/2}}{\sqrt{2\pi}} \sum_{m=0}^{\infty} \frac{a^m}{m!} x^m (1 + (-1)^m p) I_m \quad (48)$$

$$\rho_p(a)I_l = \sum_{m=0}^{\infty} (G_{lm} + p G'_{lm}) I_m \quad (49)$$

where

$$I_m = \frac{a^m}{m!} \int_0^{\infty} dy y^m e^{-y^2/2} F(y) \quad (50)$$

$$G_{lm} = \frac{1}{\sqrt{8\pi}} a^m \left( \frac{2}{1+a^2} \right)^{(l+m+1)/2} \frac{\Gamma[(l+m+1)/2]}{l!m!} \quad (51)$$

and  $G'_{lm}(a) = G_{lm}(-a)$ . In fact,  $G_{lm}$  is the matrix used for calculating the discrete persistence exponent [23], whilst  $G'_{lm}$  gives alternating persistence. This is to be expected, since for  $p = 0$  we just have ordinary persistence and for  $p \gg 1$  we would expect the paths which cross between every sampling (alternating persistence) to dominate. In the same way, one may calculate  $\rho_p(a)$  for the discretely sampled random acceleration problem studied in [24], whose stationary process is given by

$$\ddot{X} + (\alpha + \beta)\dot{X} + \alpha\beta X = \eta(T) \quad (52)$$

where  $\eta(T)$  is Gaussian white noise with mean zero and correlator  $\langle \eta(T)\eta(T') \rangle = 2\alpha\beta(\alpha + \beta)\delta(T - T')$ , and  $\alpha = 1/2$ ,  $\beta = 3/2$  for the random acceleration problem, although other values of  $\alpha$ ,  $\beta$  can be considered. We get

$$\rho_p(a)I_{ij} = \sum_{k,l=0}^{\infty} (H_{ijkl} + p H'_{ijkl}) I_{kl} \quad (53)$$

where  $H_{ijkl}$  and  $I_{ij}$  are given in [24]. Again,  $H_{ijkl}$  is the matrix used to find the discrete persistence exponent and  $H'_{ijkl}(a) = H_{ijkl}(-a)$  gives the alternating persistence exponent. We find  $\rho_p(a)$  numerically and also as a power series in  $a$  for the two processes given above. The results are shown in figures (4,5). Also the eigenfunction  $F(x)$  for the Ornstein-Uhlenbeck Process may be found by substituting the eigenvector corresponding to the largest eigenvalue into equation (48). Results for  $a = 0.5$  with  $p = 0, 0.5, 1$  are shown in figure (6).

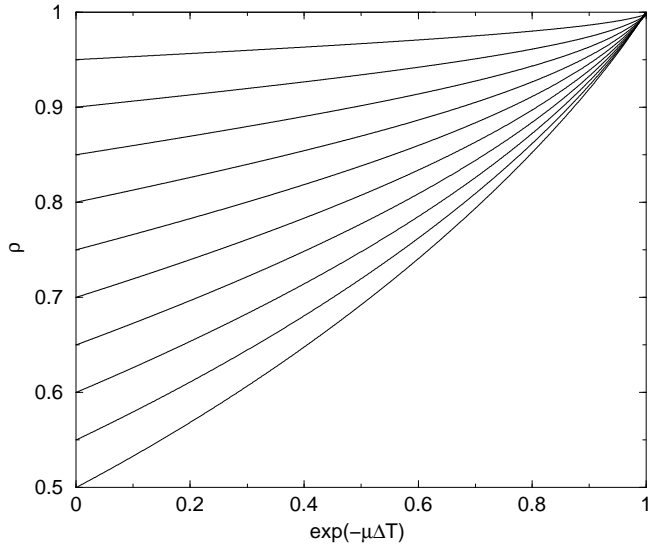


FIG. 4. Plot of the random walk discrete persistence eigenvalue  $\rho_p(a)$  for partial survival against  $a = e^{-\mu\Delta T}$  for values of the survival probability  $p$  from 0 (normal discrete persistence, lowest curve) to 1 (guaranteed to survive so  $\rho_1(a) = 1$ , top curve) in steps of 0.1. The curves are the raw series in  $a$  to order  $a^{50}$ . Note that for all the curves,  $\rho_p \rightarrow 1$  for  $a \rightarrow 1$  since a walker will always survive for a time  $\Delta T$  when  $\Delta T \rightarrow 0$ . Since the series in  $a$  are finite, they do not quite converge to 1 in this limit

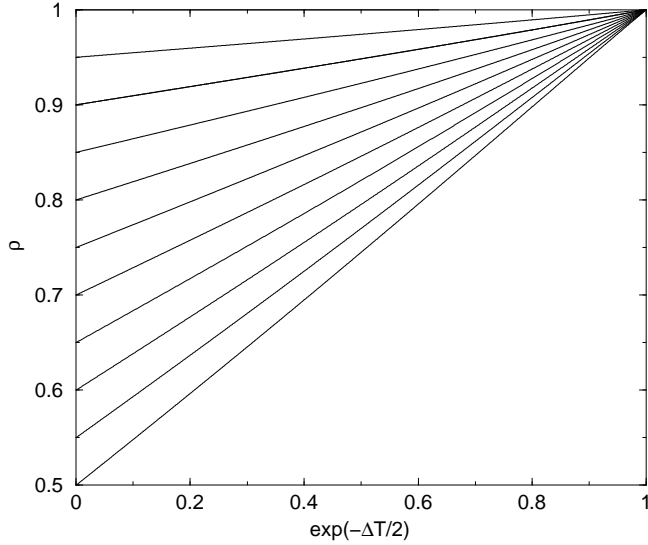


FIG. 5. Plot of the random acceleration discrete persistence eigenvalue  $\rho_p(a)$  for partial survival against  $a = e^{-\Delta T/2}$  for values of  $p$  from 0 (normal discrete persistence, lowest curve) to 1 (guaranteed to survive so  $\rho_1(a) = 1$ , top curve) in steps of 0.1. The curves are Padés of the raw series in  $a$  to order  $a^{19}$ .

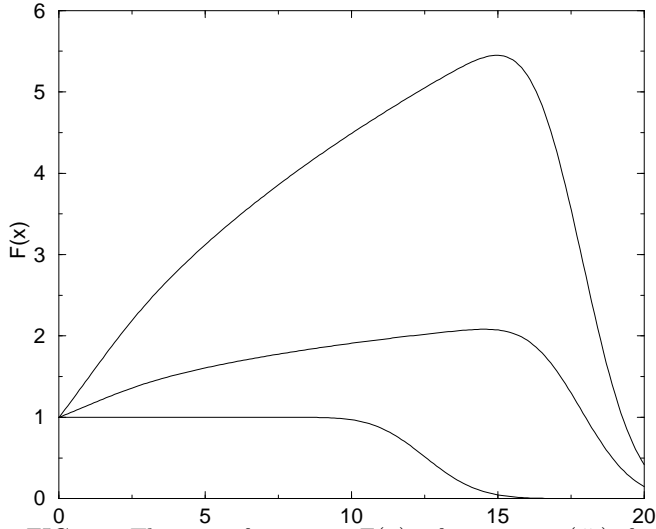


FIG. 6. The eigenfunctions  $F(x)$  of equation (47) for  $a = 0.5$  with  $p = 1$  (lowest curve),  $p = 0.5$  (middle curve) and  $p = 0$  top curve. The eigenfunctions are defined only up to an arbitrary prefactor which has been chosen here so that  $F(0) = 1$ . Since the eigenfunctions are series in  $x$ , for large  $x$  they do not converge to the correct solution. This can be clearly seen for the  $p = 1$  case where, since the walker is guaranteed to survive,  $F(x)$  is a constant everywhere whereas the plot is not constant for  $x \geq 10$ . For the  $p = 0$  case,  $F(x) \sim x^\nu$  with  $\nu = \ln \rho / \ln a$ .

So far we have found the mean and variance and also the partial-survival probability for the Ornstein-Uhlenbeck Process, a simple Gaussian Markov problem. We did this by using the propagator,  $P(Y, \Delta T | X, 0)$  (equation(12)). We also showed how the partial-survival probability of other GSPs of known propagator can be found by using the perturbative matrix method, and we illustrated this for the random acceleration problem. However, the methods used become progressively harder as the number of variables in the problem increases. The Ornstein-Uhlenbeck Process had only the position  $X$ , the random acceleration problem had  $X$  and  $V$ , while the persistence problem for the diffusion equation cannot be expressed in terms of a propagator with a finite number of variables. In the remainder of this paper we will use a different approach based on the correlator of the process  $C(T)$ . This removes the difficulties mentioned above and can, furthermore, be applied to any GSP of known correlator. The results for low-dimensional problems obtained above are slightly more accurate than those given by the correlator method because they can be calculated to higher order. They can be used as powerful checks of the accuracy of the correlator method.

## Part II

# The Correlator Expansion

The correlator expansion was initially used to calculate the discrete persistence exponent of an arbitrary Gaussian Stationary Process (GSP) and also, through extrapolation to the continuum, the continuum persistence exponent [25]. Here we will extend the method to calculate the occupation-time distribution and the distribution of crossings. As these calculations will require some explanation, we take this opportunity to describe the correlator expansion in full.

### VI. AN INTRODUCTION TO THE CORRELATOR EXPANSION

The expansion starts from the following identity for  $P_n$ , the probability of no detected crossings in  $n$  samplings:

$$P_n = \left\langle \prod_{i=1}^n \Theta[X(i\Delta T)] \right\rangle \quad (54)$$

where  $\Theta(X)$  is the Heaviside step function and the expectation value is taken in the stationary state. One may write  $\Theta[X(i\Delta T)] = (1 + \sigma_i)/2$ , where  $\sigma_i \equiv \text{sign}[X(i\Delta T)]$ , and expand the product to give,

$$P_n = \frac{1}{2^n} \left( 1 + \sum_{1=i<j}^n \langle \sigma_i \sigma_j \rangle + \sum_{1=i<j<k<l}^n \langle \sigma_i \sigma_j \sigma_k \sigma_l \rangle + \dots \right) \quad (55)$$

where the terms with odd numbers of  $\sigma$ s vanish since the process is symmetric under  $X \rightarrow -X$  (and therefore under  $\sigma \rightarrow -\sigma$ ). To evaluate the terms we use the representation

$$\sigma_l = \frac{1}{i\pi} \lim_{\epsilon \rightarrow 0} \int_{-\infty}^{\infty} \frac{dz_l z_l e^{iz_l X_l}}{(z_l - i\epsilon)(z_l + i\epsilon)} \quad (56)$$

Carrying out the required averages of the Gaussian process gives the correlation functions appearing in (55):

$$\langle \sigma_{l_1} \dots \sigma_{l_m} \rangle = \int \prod_{j=1}^m \left( \frac{dz_j}{i\pi z_j} \right) \exp \left( -\frac{1}{2} z_\alpha C_{\alpha\beta} z_\beta \right), \quad (57)$$

where  $C_{\alpha\beta} = \langle X[\alpha\Delta T] X[\beta\Delta T] \rangle = C(|\alpha - \beta|\Delta T)$ , and there is an implied summation over  $\alpha$  and  $\beta$  from 1 to  $m$ . Notice that we have already taken the limit  $\epsilon \rightarrow 0$  in (57), with the understanding that all integrals are now principal part integrals.

For the  $m = 2$  case this integral can be done exactly by differentiating with respect to  $C_{12}$  and doing the two simple Gaussian integrals before integrating again with respect to  $C_{12}$  and imposing the boundary condition that  $\langle \sigma_{l_1} \sigma_{l_2} \rangle = 0$  for  $C_{12} = 0$ . This gives the well-known result  $\langle \sigma_{l_1} \sigma_{l_2} \rangle = (2/\pi) \sin^{-1} C_{12}$ . For  $m \geq 4$  this method becomes non-trivial. Instead, we choose to expand the exponential in equation (57) in powers of  $C_{\alpha\beta}$  ( $\alpha \neq \beta$ ) leaving the terms with  $\alpha = \beta$  unexpanded (noting that  $C_{\alpha\alpha} = 1$ ). This allows us to evaluate each correlation function of the  $\sigma$ s up to a given order in the correlators  $C_{\alpha\beta}$ . By symmetry, only terms which generate odd powers of every  $z_\alpha$  in the expansion of the exponential (to give even powers overall in the integrand, through the factors  $1/z_i$ ) give a non-zero integral. This suggests a simple diagrammatic representation for the terms in (55), as given by (57). On a one-dimensional lattice containing  $n$  sites, with lattice spacing  $\Delta T$ , draw  $m$  vertices at the locations  $l_1, l_2, \dots, l_m$ . Connect the vertices by lines in all possible ways (summing over these different possibilities) subject to the constraint that each vertex is connected to an odd number of lines. Associate a factor  $\sqrt{2\pi}(p-2)!!$  (coming from evaluating the Gaussian integrals) with each vertex of order  $p$ , a factor  $(-C_{l_i l_j})^r / r!$  with the  $r$  lines connecting site  $l_i$  to site  $l_j$ , and an overall factor  $(\pi i)^{-m}$  with the diagram. This suffices to evaluate the integrals in (57). Evaluating the summations in (55) involves enumerating all configurations of the vertices on the lattice for a given ordering of the points, and noting that the factor  $C_{l_i l_j}$  associated with a given line is equal to  $C(q\Delta T)$ , where  $q = |l_i - l_j|$  is the length of the line in units of  $\Delta T$ .

We choose to define  $C(\Delta T)$  as  $1^{st}$  order small and  $C(q\Delta T)$  as  $q^{th}$  order small. Although somewhat arbitrary, this is a large  $\Delta T$  expansion and most processes of physical interest have correlators  $C(q\Delta T)$  which decrease exponentially for large argument, so our definition is consistent for large  $\Delta T$ . For the random walk, the correlator is  $C(T) = e^{-\Delta T/2}$

and the definition is always valid. For other processes it is often possible to re-expand the correlator in terms of an exponential and work to a given order (in practice we can go up to 14th order) in this exponential. This can be done for, e.g., the random acceleration problem. The order of a diagram is then equal to the total length of its lines (measured in units of the lattice spacing  $\Delta T$ ). Thus to a given order  $k$ , we need only evaluate correlations functions with separations up to  $2k \Delta T$ .

To illustrate this approach, we show in Figure 7 all the topologically distinct diagrams contributing to  $\langle \sigma_i \sigma_j \sigma_k \sigma_l \rangle$  up to 4<sup>th</sup> order. The first diagram, when enumerated on the lattice, will be 2<sup>nd</sup> order or greater, while the remaining five will be 4<sup>th</sup> order or greater.

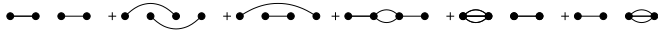


FIG. 7. All topologically distinct contributions to  $\langle \sigma_i \sigma_j \sigma_k \sigma_l \rangle$  up to fourth order. Note that the 1st, 5th and 6th diagrams are disconnected, whilst the others (including diagrams 2 and 3) are connected (due to the constraint that the order of the points  $i, j, k, l$  must be unchanged).

In Figure 8 are shown the enumerations of two of the basic diagrams of figure 7 together with their embedding factors (the number of ways they can be placed on the lattice), up to 5th order.

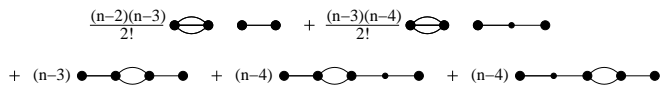


FIG. 8. Enumeration of two of the diagrams from figure 7, with embedding factors, up to fifth order. Large dots are vertices, small dots intermediate sites. The final diagram here gives a contribution  $(n-4)(2/\pi^2)C(2\Delta T)C(\Delta T)^3$  to  $P_n$ .

Thus the calculation of  $P_n$  proceeds in 3 stages:

- 1: all the basic diagrams up to the required order are found, for example the 4-vertex diagrams shown in figure 7.
- 2: the basic diagrams are enumerated on the lattice, including the ‘stretched’ diagrams, as shown in figure 8.
- 3: the appropriate factors are assigned to each diagram.

The total number of enumerated diagrams increases roughly by a factor of 2 for each extra order. At 14th order there are 12 434 diagrams. The process was automated using MATHEMATICA. For calculating  $P_n$ , finding the basic diagrams was the most challenging task in terms of computer time and memory. To achieve 14th order we used the fact that all disconnected diagrams can be constructed by combining two or more connected diagrams. At 14th order, diagrams with 12 or more vertices are disconnected, thus only connected diagrams with up to 10 vertices need be found. Furthermore, diagrams containing 2 or more lines connecting the same points can be constructed from diagrams with only 0 or 1 lines connecting points by adding pairs of lines. The procedure adopted was as follows:

For the 2 to 10-vertex diagrams: all possible diagrams up to 14th order with only 0 or 1 lines connecting points *and* all vertices odd are constructed. To these diagrams pairs of lines are added in all possible ways up to 14th order. The connected diagrams are then selected and stored.

For 2 to 28-vertex diagrams: all diagrams are constructed by combining the connected diagrams found above, for example, the 6-vertex diagrams are formed from 3 2-vertex diagrams, one 2-vertex and one 4-vertex diagrams, and one 6-vertex diagram (with the appropriate permutation factors arising from the various ways of ordering the connected diagrams). For large vertex numbers, this produces significant savings over naively trying all diagrams (since the vast majority of diagrams do not satisfy the odd-vertex criterion). In this way, up to order  $k$  we need only find all connected diagrams with up to  $q$  vertices, where  $q = (2k + 4)/3$  is even and we round down, whilst the diagrams go up to  $2k$  vertices.

Having found  $P_n$ , we find  $\rho (= e^{-\theta \Delta T})$  using the fact that  $P_n \sim \rho^n$  for large  $n$ . Thus  $\rho$  is formally obtained as  $\rho = \lim_{n \rightarrow \infty} P_{n+1}/P_n$ . However, since we started in the stationary state, the relation  $\rho = P_{n+1}/P_n$  in fact holds for all  $n$  larger than the length of the longest diagram. Expanding the expression for  $P_{n+1}/P_n$  as a Taylor series up to 14th order in  $a = e^{-\Delta T/2}$  gives us a series expansion for  $\rho(a)$  about  $\Delta T = \infty$  ( $a = 0$ ). For the random walk, for example,  $C(\Delta T) = e^{-\Delta T/2} = a$  for  $\mu = 1/2$ , substituting this into our expression for  $\rho$  gives us a series up to 14th order in  $a$  whose coefficients agree with those of the matrix method (to within the numerical error of the matrix method).

For the usual random acceleration problem,  $C(\Delta T) = (3e^{-\Delta T/2} - e^{-3\Delta T/2})/2 = (3a - a^3)/2$ . For this case our identification of  $C(14\Delta T)$  as being of the same order as  $C(\Delta T)^{14}$  does not hold for all  $\Delta T$ . However, if we only keep terms up to  $a^{14}$  our expansion be exact up to order 14 in  $a$ . Whenever possible, this is what we will always do. Note that in this way we are now working strictly to 14th order, even though  $C(j\Delta T) \neq C(\Delta T)^j$ .

In [23] we introduced the concept of alternating persistence, with  $P_n^A$  being the probability that  $X_i$  is positive for odd  $i$  and negative for even  $i$  (or vice versa). We find  $\rho_A$  by noting that, whereas before we required  $X_1, X_2, \dots, X_n > 0$ , we now require  $X_1, -X_2, X_3, -X_4 \dots X_n > 0$ . Thus the calculation is as before except that  $C(q\Delta T) \rightarrow -C(q\Delta T)$  for  $q$  odd. Making this minor change to the normal persistence result gives us the alternating persistence exponent. This way of accounting for sign changes between  $X_i, X_j$  will be used below to calculate the distribution of crossings.

We have applied the correlator expansion to the random walk,  $\dot{x} = \eta(t)$  and random acceleration,  $\ddot{x} = \eta(t)$  using the transformation to logarithmic time to generate the corresponding stationary processes. Furthermore we have studied diffusion from random initial conditions in 1-3 dimensions,  $\partial\phi/\partial t = \nabla^2\phi$ , where  $\phi(\mathbf{x}, t)$  is the diffusion field and the initial condition  $\phi(\mathbf{x}, 0)$  is delta-correlated Gaussian noise. We consider the persistence of  $\phi$  at a single site, for example  $\phi(\mathbf{0}, t)$ . For this process the correlator is:

$$C(T) = \text{sech}^{d/2}(T/2) \quad (58)$$

where  $d$  is the space dimension. As for the random acceleration, we define  $a = \exp(-\Delta T/2)$  for  $d = 2$  and  $a = \exp(-\Delta T/4)$  for  $d = 1, 3$  and then expand the correlator in powers of  $a$ . For  $d = 1, 2$  the lowest power of  $a$  is  $a^1$  and so we expand up to  $a^{14}$  whilst for  $d = 3$  the lowest power is  $a^3$  and so we expand up to  $a^{42}$ . We also considered the processes  $d^n x/dt^n = \eta(t)$  for  $n > 3$ . In logarithmic time the correlators are [20]:

$$C_n(T) = (2 - 1/n)e^{-T/2} {}_2F_1(1, 1 - n; 1 + n; e^{-T}) \quad (59)$$

where  ${}_2F_1$  is the standard hypergeometric function. The  $n = 1, 2$  cases are the random walk and random acceleration, whilst the limit  $n \rightarrow \infty$  case reproduces the correlator for the  $d = 2$  diffusion process mentioned above [20].

For all these problems we define a discrete persistence exponent,  $\theta_D(a) = -\ln \rho(a)/\Delta T = \ln \rho(a)/2 \ln a$ , and plot  $\theta_D(a)$  against  $a$  for  $0 \leq a \leq 1$ , i.e.  $\infty \geq \Delta T \geq 0$ . Since we are plotting finite series in powers  $a$ , they do not converge for  $a \rightarrow 1$ . This problem is exacerbated by the  $1/\ln a$  term in the definition of  $\theta_D(a)$ , which causes  $\theta_D(1)$  to blow up unless  $\rho(1) = 1$ . To make  $\rho$  and hence  $\theta_D(a)$  more accurate for  $a$  close to 1 we extrapolate  $\theta_D(a)$  to the continuum. To do this we use the technique of Padé approximants borrowed from the field of series expansions for critical phenomena [27]. The Padé approximant involves replacing the 14th order series in  $a$  with a fraction whose numerator and denominator are series in  $a$ . The sum of the order of these two series is 14 and the coefficients are chosen so that when the fraction is expanded as a series in  $a$  it is identical to the raw series. This approach markedly improves the results for  $\rho$ . For example, for the random walk, the Padé of the 14th order series appears to better the 25th order raw series obtained from the matrix method (both raw series agree, of course, up to 14th order). However, in order to get accurate continuum results for  $\theta$  we add 1 further term to the Padé (either numerator or denominator) whose coefficient is chosen so that the exact constraint  $\rho(1) = 1$  is satisfied. This serves to give reasonably accurate estimates of the continuum persistence exponent. For example, for the random acceleration problem we find  $\theta = 0.2506(5)$  from the Padé approach, compared to the exact result of  $1/4$ .

For certain sufficiently smooth processes the derivative of  $\theta_D(\Delta T)$  at  $\Delta T = 0$  is zero [24]. We can thus add a further term to the Padé to impose this constraint, and markedly improve the accuracy of our estimate of the continuum  $\theta$ . The diffusion equation in all dimensions and the  $d^n x/dt^n = \eta(t)$  processes for  $n \geq 3$  are all suitable. Table VI shows the continuum results for diffusion in 1-3 dimensions as reported in [25], with numerical results and also the singly constrained and IIA results for comparison. For  $d = 1$  the IIA is slightly better, but the correlator expansion is more accurate for  $d = 2, 3$ . Furthermore, we obtain estimates of the errors and, by going to higher order we may improve our results. Table VI shows the continuum results for the  $d^n x/dt^n = \eta(t)$  processes with  $3 \leq n \leq 10$ . Figure 9 shows how  $\theta_n$  varies with  $n$ . Notice in particular that  $\theta_n - \theta_\infty \propto 1/n$  for  $n > 20$ , and that  $\theta_\infty$  is identical to that of 2-d diffusion (since the correlators are identical).

	Padé1CR	Padé2CR	numerical	IIA
$\ddot{x}$	0.2506(5)	...	1/4 (exact)	0.2647
1-d diff	0.119(1)	0.1201(3)	0.12050(5)	0.1203
2-d diff	0.187(1)	0.1875(1)	0.1875(1)	0.1862
3-d diff	0.24(3)	0.237(1)	0.2382(1)	0.2358

Table VI. Results for the continuum persistence exponent  $\theta$  for the random acceleration problem and the diffusion equation in 1-3 dimensions. Padé1CR is the Padé results with 1 constraint, Padé2CR has 2 constraints. Numerical [13] and IIA results are shown for comparison.

n	Padé2CR	IIA
3	0.22022(3)	0.22283
4	0.20958(3)	0.21029
5	0.20413(3)	0.20417
6	0.20084(3)	0.20054
7	0.19864(3)	0.19813
8	0.19707(3)	0.19642
9	0.19589(3)	0.19514
10	0.19496(3)	0.19414

Table VI. Results for  $\theta_n$  against  $n$  for small  $n$ . The Padé correlator expansion with 2 constraints is shown along with the Independent Interval Approximation. The Padé results are an average of suitable Padés of order 14 to 10. Note that for  $n = 2$  (the random acceleration problem), the IIA gives  $\theta = 0.2647$  whilst the analytical result is  $1/4$ . For  $n \rightarrow \infty$  (the diffusion equation), the Padé result with 2 constraints is  $0.1875(1)$ , the numerical result is  $0.1875(1)$  and the IIA result is  $0.1862$ .

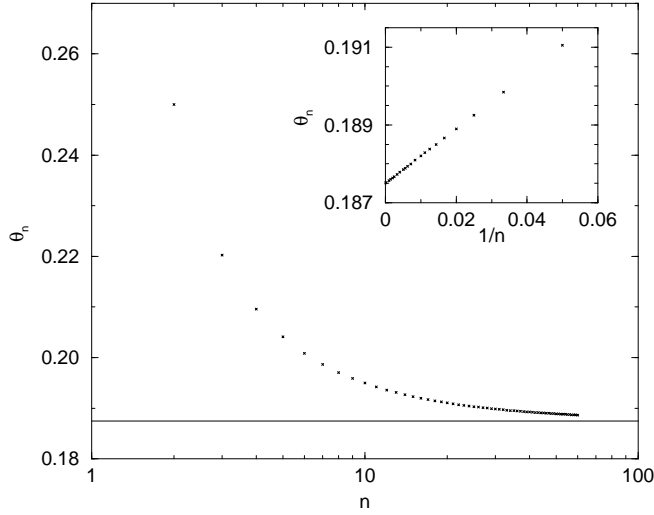


FIG. 9. Plot of  $\theta_n$  against  $n$  for small  $n$ . The  $n = 1, 2$  results are omitted as they are known analytically to be  $1/2$  and  $1/4$  respectively and only one constraint may be imposed on the Padé in these cases. Note that  $\theta_n$  goes to the continuum result of  $0.1875(1)$  (solid line) rather slowly, in fact as  $1/n$ , see inset. The results were obtained using Padés with 2 constraints, an average being taken of suitable Padés of order 14 to 10. Inset: Plot of  $\theta_n$  against  $1/n$  showing that  $\theta_n - \theta_\infty \propto 1/n$  for  $n > 20$ .

And so, by the use of these two constraints we have been able to extend a series expansion about  $\Delta T = \infty$  all the way to the  $\Delta T \rightarrow 0$  limit. The ability to do this does however depend on the correlator. First, if the process is ‘rough’, i.e.  $1 - C(T) \propto T^\beta + \dots$  with  $0 < \beta < 2$ , so that the probability distribution of the time  $T$  between two zero-crossings behaves as  $P_1(T) \propto T^\alpha + \dots$ , with  $\alpha < 0$ , then we have shown [24] that  $\theta(0) - \theta(\Delta T) \sim \Delta T^{1+\alpha}$  for small  $T$ . For the random walk, for example,  $\alpha = -1/2$  and so we get a square root cusp in  $\theta_D(\Delta T)$  for  $\Delta T \rightarrow 0$  which the series expansion about  $\Delta T = \infty$  cannot reproduce. Consider processes such as

$$\frac{\partial h}{\partial t} = -(-\nabla^2)^{z/2} h + \eta(t) \quad (60)$$

describing linear interface growth, where  $\eta(\mathbf{x}, t)$  is delta correlated in space and time. The normalized autocorrelation function of  $h(x, t)$  has, for  $d < z$ , the form

$$C(T) = \cosh(T/2)^{2\beta} - |\sinh(T/2)|^{2\beta} = 1 - |T/2|^{2\beta} + \dots \quad (61)$$

where  $T = \ln t$  as usual,  $\beta = (1/2)(1 - d/z)$  and  $d$  is the spatial dimension [28]. Since  $\beta < 1/2$  this process will always be ‘rough’, so extrapolation of the series to the continuum limit is not possible. Secondly, the correlator may not be



easily expandable in some suitable variable such as the  $e^{-\Delta T/2}$  used earlier. Another process, fractional Brownian motion, defined as a Gaussian process  $x(t)$  with stationary increments  $\langle [x(t) - x(t')]^2 \rangle \propto |t - t'|^{2\beta}$ , has normalized correlator [29]

$$C(T) = \cosh(\beta T) - \frac{1}{2} \left| 2 \sinh \left( \frac{T}{2} \right) \right|^{2\beta}, \quad (62)$$

where  $T = \ln t$  as usual. For general  $\beta$  there are two incommensurate variables  $e^{-\beta \Delta T}$  and  $e^{-\Delta T/2}$ , making it difficult to construct a controlled expansion.

Finally, when applying the 2 constraints to the 3-dimensional diffusion problem, we have been unable to numerically solve the 44 simultaneous nonlinear equations required to construct the expansion to  $O(a^{42})$ . Thus we have only gone up to  $a^{29}$  in this problem. This is not however an insuperable difficulty.

Note however that, even when we cannot get continuum results, for  $\Delta T$  large the expansion will always work, as just substituting in the raw correlator is good enough.

Having introduced the correlator expansion for the calculation of persistence exponents, in the following sections we will extend it to calculate properties of the occupation-time and crossing-number distributions.

## VII. OCCUPATION-TIME DISTRIBUTION

The occupation-time distribution, considered for the continuous case in [9–11], is the probability distribution  $R(\tau(T))$ , where

$$\tau(T) = \frac{1}{T} \int_0^T dT' \Theta(X(T')) \quad (63)$$

and  $\Theta(X)$  is the Heaviside step function. For a symmetric distribution of zero mean,  $R_T(\tau)$  is symmetric about  $\tau = 1/2$ . Then  $R_T(0)$  and  $R_T(1)$  give the persistence probability  $P(T)$  introduced earlier. The discrete-sampling equivalent,  $R_{n,s}$ , is the probability that  $X(T)$  has been found to be positive at exactly  $s$  out of the  $n$  samplings. Thus,

$$s(n)/n = r(n) = \frac{1}{n} \sum_{i=1}^n \Theta[X(i\Delta T)]. \quad (64)$$

Writing  $\Theta[X(i\Delta T)] = (1 + \sigma_i)/2$ , where  $\sigma_i \equiv \text{sign}[X(i\Delta T)]$ , we get

$$\langle r(n) \rangle = \frac{1}{2} \quad (65)$$

and

$$\langle r(n)^2 \rangle = \frac{1}{4} + \frac{1}{2\pi n^2} \sum_{i=1}^n \sum_{j=1}^n \sin^{-1}[C(|i-j|\Delta T)] \quad (66)$$

where we have used the result that  $\langle \sigma_i \sigma_j \rangle = (2/\pi) \sin^{-1}[C(|i-j|\Delta T)]$ . If we choose as before to work to a given order in the correlator, we need only evaluate the sum up to that order. Taking the large  $n$  limit, we can change the sum to:

$$\langle r(n)^2 \rangle = \frac{1}{4} + \frac{1}{4n} + \frac{1}{\pi n} \sum_{k=1}^o \sin^{-1}[C(k\Delta T)] \quad (67)$$

where  $o$  is the order to which we wish to work. It has been pointed out [16] that for  $n$  large, the widely separated (in time) parts of the time series become uncorrelated and, following the central limit theorem,  $R_{n,s}$  is Gaussian for  $s$  close to  $1/2$  with standard deviation given by equation (67). We will use this as a check of our final result for  $R_{n,s}$ .

To find  $R_{n,s}$  we must sum over all ‘paths’ involving  $s$  positive samplings (and  $n-s$  negative ones). So the probability,  $R_{n,s}$ , to find  $s$  positive values from  $n$  samplings is

$$R_{n,s} = \left\langle \delta_{2s-n, \sum_i \sigma_i} \right\rangle = \left\langle \frac{1}{2^n} \sum_{\{\epsilon_i = \pm 1\}} \delta_{2s-n, \sum_i \epsilon_i} \prod_{i=1}^n (1 + \epsilon_i \sigma_i) \right\rangle \quad (68)$$

where  $\delta_{\alpha,\beta}$  is the Kronecker delta function which we choose to write in analytic form as a Cauchy integral

$$\delta_{\alpha,\beta} = \frac{1}{2\pi i} \oint \frac{dz}{z^{\alpha-\beta+1}}, \quad (69)$$

where the integration contour encircles the origin. Substituting this into eqn. (68) gives,

$$R_{n,s} = \frac{1}{2\pi i} \oint \frac{dz}{z^{2s-n+1}} \left\langle \frac{1}{2^n} \sum_{\{\epsilon_i=\pm 1\}} \prod_{i=1}^n z^{\epsilon_i} (1 + \epsilon_i \sigma_i) \right\rangle. \quad (70)$$

Summing over the  $\epsilon_i$ s gives:

$$R_{n,s} = \frac{1}{2\pi i} \oint \frac{dz}{z^{2s-n+1}} \left( \frac{1+z^2}{z} \right)^n \left\langle \frac{1}{2^n} \prod_{i=1}^n \left( 1 + \frac{z^2-1}{z^2+1} \sigma_i \right) \right\rangle. \quad (71)$$

The term which is averaged over is identical to that of the normal persistence calculation apart from the factor  $(z^2-1)/(z^2+1)$  associated with each  $\sigma_i$ . Making this minor change to the previous calculation of persistence gives us a term  $\tilde{\Upsilon}^n(z)$  where before we had  $\rho^n$ , and so  $\tilde{\Upsilon}(\infty) = \rho$ . Replacing  $s$  by  $rn$  where  $0 \leq r \leq 1$  and anticipating that  $R_{n,s} \sim [\rho(r)]^n$  for  $n$  large gives us an expression for  $\rho(r)$  which we can evaluate by steepest descents:

$$[\rho(r)]^n = \frac{1}{2\pi i} \oint \frac{dt}{2t} \exp[n(\ln(1+t) - r \ln t + \ln \Upsilon(t))] \quad (72)$$

where we have replaced  $z^2$  by  $t$ , and  $\Upsilon(t) = \tilde{\Upsilon}(\sqrt{t})$ . As a simple check, at zeroth order  $\Upsilon$  is  $1/2$  and the method of steepest descents gives a saddle-point value  $t_s^{(0)} = r/(1-r)$ , and

$$R_{n,s} \sim \frac{1}{2^n} \exp\{-n[r \ln r + (1-r) \ln(1-r)]\}. \quad (73)$$

This is the same as the combinatorial result,

$$R_{n,s} = \frac{1}{2^n} \binom{n}{rn} \quad (74)$$

when expanded to leading order for large  $n$  using Stirling's formula. Note that there is hence also a  $\sqrt{n}$  term in  $R_{n,s}$  which we ignore relative to the exponential for  $n \rightarrow \infty$ .

We use the method of steepest descents in the following way. Having found the position  $t_s^{(0)}$  of the saddle point to zeroth order, we substitute it into the right-hand side of the general saddle-point equation

$$t_s = \frac{r}{1-r} - \frac{t_s(1+t_s)}{1-r} \Upsilon'(t_s), \quad (75)$$

where  $\Upsilon'(t) \equiv d\Upsilon/dt$ , and thus find  $t_s$  to first order, and so on recursively up to 10th order. Substituting  $t_s$  into the exponent of equation (72) gives an analytic expression for  $R_{n,s}$  in the large  $n$  limit and hence  $\rho(r)$ . Just as in the expression for persistence, the expression for  $\rho(r)$  is rather long and it was only possible to find  $\rho(r)$  analytically to 10th order.

As stated in the previous section, for  $r$  close to  $\langle r \rangle = 1/2$ ,  $\rho(r)$  approximates to a gaussian distribution,

$$\rho(r) \propto \exp \left[ -\frac{1}{2n} \frac{(r - \langle r \rangle)^2}{\langle r^2 \rangle - \langle r \rangle^2} \right]. \quad (76)$$

Thus one expects that the quantity  $\lim_{r \rightarrow \langle r \rangle} (r - \langle r \rangle)^2 / [-2n \ln \rho(r)]$  should equal the variance of  $r$  calculated previously, and indeed these two quantities agree term by term to 10th order, providing a useful cross-check.

We apply our result to the random walk, random acceleration, and diffusion from random initial conditions in 1-3 dimensions. We recall that  $R_{n,s}$  is the probability for  $n$  measurements of  $X$  to return  $s$  positive values. We have shown that for  $n \rightarrow \infty$ ,  $s \rightarrow \infty$  with  $r = s/n$  fixed it has the form  $R_{n,s} \sim [\rho(r)]^n$ , which can be written in the alternative form  $R_{n,s} \sim \exp[-\theta_D(r)T]$ , where  $T = n\Delta T$  as usual and  $\theta_D = -\ln \rho(r)/\Delta T$ .

Plots of  $\theta_D(r)$  against  $r$  for various values of  $\Delta T$  are shown in figures 11, 12, 13, 14 and 15. For the diffusion equation we are able to Padé the series and apply 2 constraints, giving us good estimates for the continuum  $\theta(r)$ , i.e. the limiting value of  $\theta_D(r)$  as  $\Delta T \rightarrow 0$ . Plots of  $\theta(r)$  are also shown in figure 10. The second constraint, that  $d\theta(r)/d\Delta T|_{\Delta T=0} = 0$  for sufficiently smooth processes (including diffusion), comes from a similar argument to that given earlier [24] for standard persistence: as  $\Delta T$  is increased from zero, the first correction to  $\theta$  comes from the contribution of a path that is the same as a contributing path in the continuum, apart from one undetected double crossing which (to lowest order in  $\Delta T$ ) gives a correction to  $\theta$  of order  $\Delta T^2$  and thus  $d\theta(r)/d\Delta T|_{\Delta T=0} = 0$ .

The function  $\theta(r)$  is the large-deviation function for the occupation-time distribution. Close to  $r = \langle r \rangle = 1/2$ , it is quadratic in  $r - \langle r \rangle$ . The probability distribution  $P_r(r)$  of  $r$  is given by  $P_r(r) \propto [\rho(r)]^n = \exp[-(1/2)(r - \langle r \rangle)^2 / (\langle r^2 \rangle - \langle r \rangle^2)]$  for  $r$  near  $\langle r \rangle$ . This means that the typical fluctuations in  $r$  around the mean are of order  $n^{-1/2}$  for large  $n$  since the variance is proportional to  $1/n$ . The full function  $\theta(r)$  is required to determine the probability of large deviations from the mean, where the fluctuations are non-Gaussian.

We end this section by noting that the full large deviation function  $\theta_D(r)$  associated with the occupation-time distribution was computed analytically [18] for the intrinsically discrete process

$$\psi_i = \cos(\omega)\phi_i + \sin(\omega)\phi_{i-1} , \quad (77)$$

where the  $\phi_i$  are independently distributed gaussian random variables. This process appears as a limiting case of the diffusion equation on a hierarchical lattice [30] and also appears in the one dimensional Ising spin glass problem [18,31]. Exact results were obtained for the case  $\omega = \pi/4$ . Interestingly, these results turn out to be independent of the distribution of  $\phi_i$  provided that it is symmetric. We have also obtained the the large deviation function for  $\omega = \pi/4$  by the correlator method. The comparison with the exact results is shown in figure 16.

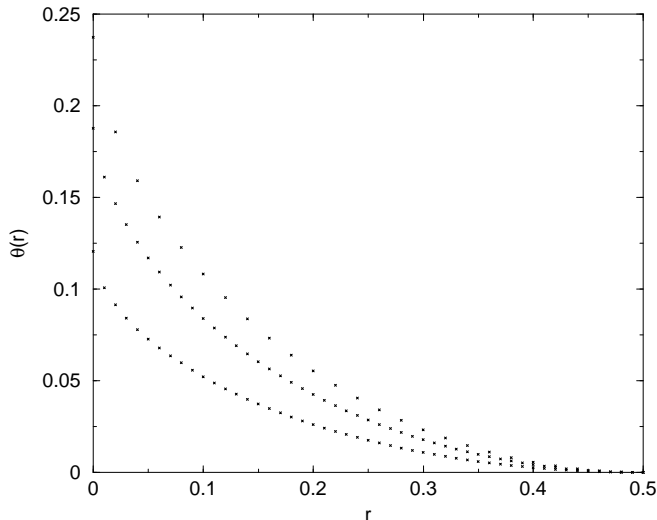


FIG. 10. Plot of the continuum large deviation function  $\theta(r)$  against  $r$  for the diffusion equation in 1, 2 and 3 dimensions (bottom to top respectively).  $\theta(r)$  is symmetric about  $r = 1/2$ . The results were obtained using Padés with 2 constraints, an average being taken of suitable Padés of order 10 to 7 for 1 and 2 dimensions and of order 7 to 6 for 3 dimensions.

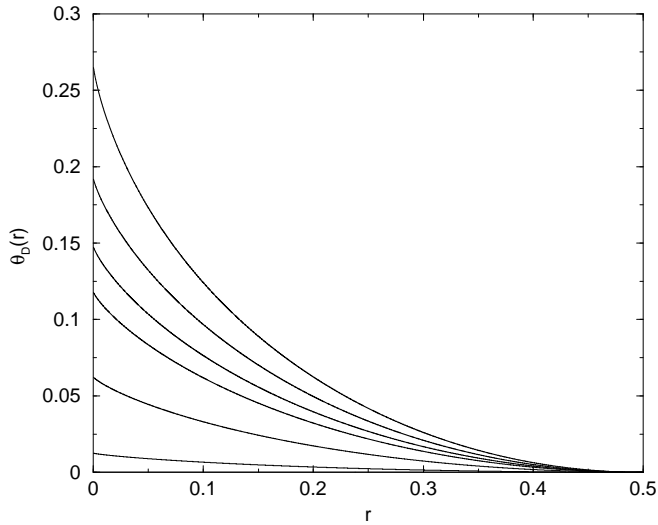


FIG. 11. Plot of  $\theta_D(r)$  against  $r$  for the random walk with  $\exp(-\Delta T/2) = 1/2, 1/4, 1/8, 1/16, 1/256$  and  $1/2^{40}$  (top to bottom respectively). The curves were plotted from the raw series in  $\exp(-\Delta T/2)$  to 10th order. Note that  $r = 0, 1$  corresponds to ordinary discrete persistence and that the curves are symmetric about  $r = 1/2$ .

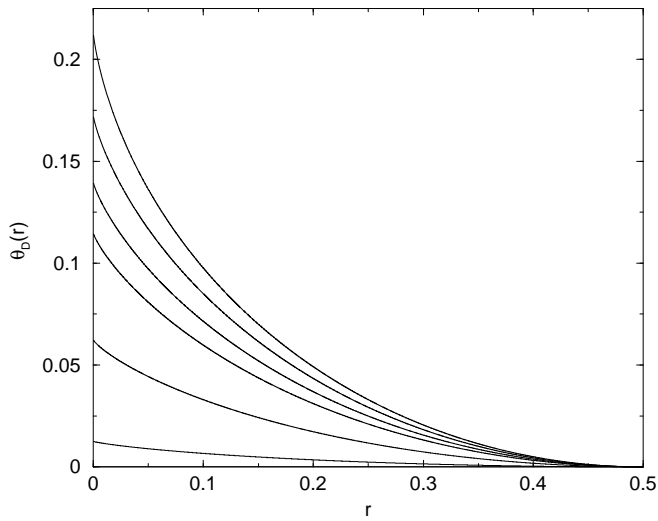


FIG. 12. Plot of  $\theta_D(r)$  against  $r$  for the random acceleration with  $\exp(-\Delta T/2) = 1/2, 1/4, 1/8, 1/16, 1/256$  and  $1/2^{40}$  (top to bottom respectively). The curves were plotted from the raw series in  $\exp(-\Delta T/2)$  to 10th order. Note that  $r = 0, 1$  corresponds to ordinary discrete persistence and that the curves are symmetric about  $r = 1/2$ .

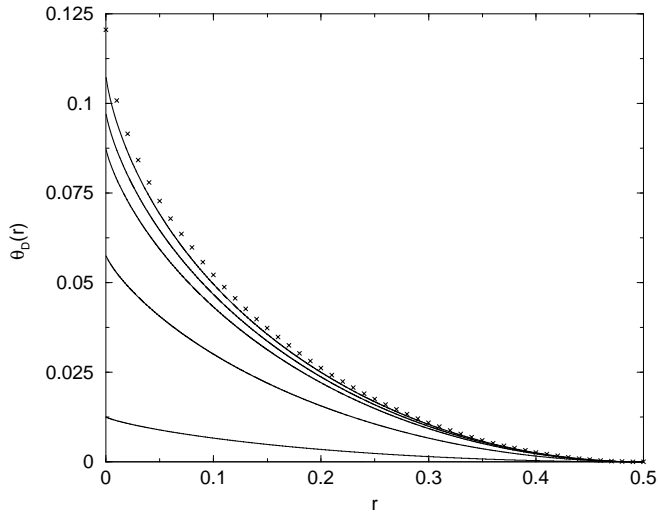


FIG. 13. Plot of  $\theta_D(r)$  against  $r$  for diffusion in 1 dimension with  $\exp(-\Delta T/2) = 1/4, 1/8, 1/16, 1/256$  and  $1/2^{40}$  (top to bottom respectively). The curves were plotted from the raw series in  $\exp(-\Delta T/2)$  to 10th order. The  $\exp(-\Delta T/2) = 1/2$  curve is not shown as the raw series had not converged at 10th order. Also shown are the results for the continuum limit from figure 10. Note that  $r = 0, 1$  corresponds to ordinary discrete persistence and that the curves are symmetric about  $r = 1/2$ .

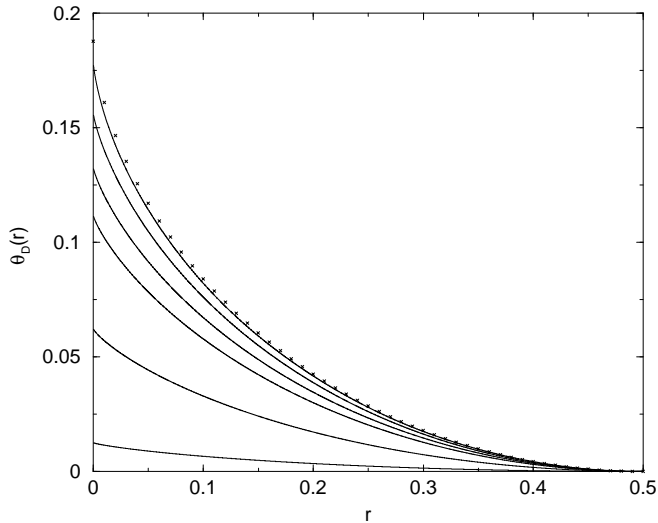


FIG. 14. Plot of  $\theta_D(r)$  against  $r$  for diffusion in 2 dimension with  $\exp(-\Delta T/2) = 1/2, 1/4, 1/8, 1/16, 1/256$  and  $1/2^{40}$  (top to bottom respectively). The curves were plotted from the raw series in  $\exp(-\Delta T/2)$  to 10th order. Also shown are the results for the continuum limit from figure 10. Note that  $r = 0, 1$  corresponds to ordinary discrete persistence and that the curves are symmetric about  $r = 1/2$ .

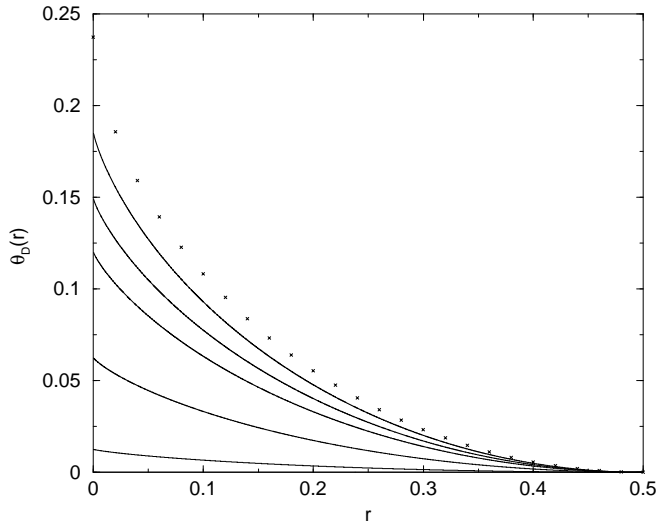


FIG. 15. Plot of  $\theta_D(r)$  against  $r$  for diffusion in 3 dimension with  $\exp(-\Delta T/2) = 1/4, 1/8, 1/16, 1/256$  and  $1/2^{40}$  (top to bottom respectively). The curves were plotted from the raw series in  $\exp(-3\Delta T/2)$  to 10th order. The  $\exp(-\Delta T/2) = 1/2$  curve is not shown as the raw series had not converged at 10th order. Also shown are the results for the continuum limit from figure 10. Note that  $r = 0, 1$  corresponds to ordinary discrete persistence and that the curves are symmetric about  $r = 1/2$ .

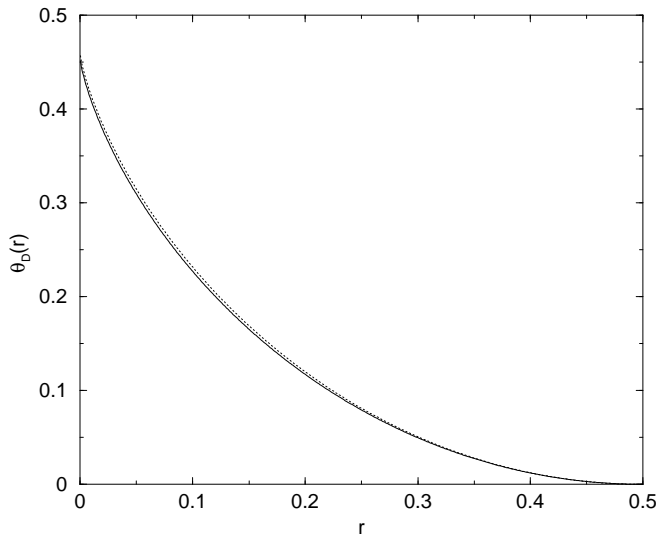


FIG. 16. Plot of  $\theta_D(r)$  against  $r$  for the intrinsically discrete process  $\psi_i = (\phi_i + \phi_{i-1})/\sqrt{2}$  where the  $\phi_i$ s are independent identically distributed symmetric random variables. The curves show the raw correlator result to 10th order (dotted line) and the exact result [18] (solid line). The curves differ by a maximum of 0.00575. Note that  $r = 0, 1$  corresponds to ordinary discrete persistence and that the curves are symmetric about  $r = 1/2$ .

### VIII. OCCUPATION-TIME PARTIAL SURVIVAL

Here we consider the discrete occupation-time partial-survival probability,  $R_n(p)$ . Let us suppose that the process ‘dies’ with probability  $1 - p$  whenever  $X$  is sampled to be positive. Then  $R_n(p)$  is defined to be the probability of the process surviving  $n$  samplings if the variable  $X_i$  survives being sampled as positive with probability  $p$ . Samplings as negative are always survived. Thus,

$$R_n(p) = \sum_{s=0}^n p^s R_{n,s} \quad (78)$$

and so  $R_n(p)$  is also the generating function for  $R_{n,s}$  since

$$R_{n,s} = \frac{1}{s!} \left. \frac{d^s}{dp^s} R_n(p) \right|_{p=0} \quad (79)$$

or alternatively

$$R_{n,s} = \oint \frac{dp}{p^{s+1}} R_n(p) \quad (80)$$

Also, writing  $p^s$  as  $\exp(s \ln p)$  and expanding the exponentials gives:

$$\ln \rho^r(p) = \sum_{j=1}^{\infty} \frac{\ln p^j}{j!} \langle s^j \rangle_c \quad (81)$$

where  $\langle s^j \rangle_c$  is the  $j$ th cumulant of the occupation time,  $s$ , and we have used  $R_n(p) = [\rho(p)]^n$ , which, as for persistence (but unlike  $R_{n,s}$ ) is true for any  $n$  provided that  $n$  is larger than the largest diagram involved in the evaluation of  $R_n(p)$ . Thus calculating  $R_n(p)$  gives us another method for finding the moments of the number of crossings and also  $R_{n,s}$  although the evaluation of  $R_{n,s}$  by the contour integration is entirely equivalent to the previous method and differentiating  $R_n(p)$   $s$  ( $= rn$ ) times becomes unfeasible for large  $n$ .

$R_n(p)$  is found in a similar way to before, by summing over all possible ‘paths’,

$$R_n(p) = \left\langle \frac{1}{2^n} \sum_{\epsilon_i = \pm 1} \prod_{i=1}^n \begin{cases} p(1 + \sigma_i), & \epsilon_i = 1 \\ (1 - \sigma_i), & \epsilon_i = -1 \end{cases} \right\rangle, \quad (82)$$

where  $\sigma_i = \text{sgn}(X_i)$  as usual, and the average is over the variables  $X_i$  ( $i = 1, \dots, n$ ). Thus we get

$$R_n(p) = \left\langle \frac{1}{2^n} (p+1)^n \prod_{i=1}^n \left( 1 + \frac{p-1}{p+1} \sigma_i \right) \right\rangle \quad (83)$$

which is the same as the calculation for normal persistence except that we include a factor  $(p-1)/(p+1)$  with each  $\sigma_i$  and an overall factor  $(p+1)^n$ . Thus we can find  $\rho(p) = \exp[-\theta(p)]$  to order 14. This is done and results for diffusion in 1-3 dimensions are shown in figures (17, 18, and 19). Note that, for  $\Delta T \rightarrow 0$ , a positive excursion by the underlying continuous process will survive with zero probability since the number of samplings  $\rightarrow \infty$ . Thus  $\theta(p)|_{\Delta T=0}$  is just the continuum persistence exponent. It is therefore possible to improve  $\theta(p)$  for  $\Delta T$  small by applying  $\theta(p)|_{\Delta T=0} = \theta$  as a constraint, in addition to the standard constraint  $\rho(p)|_{\Delta T=0} = 1$ .

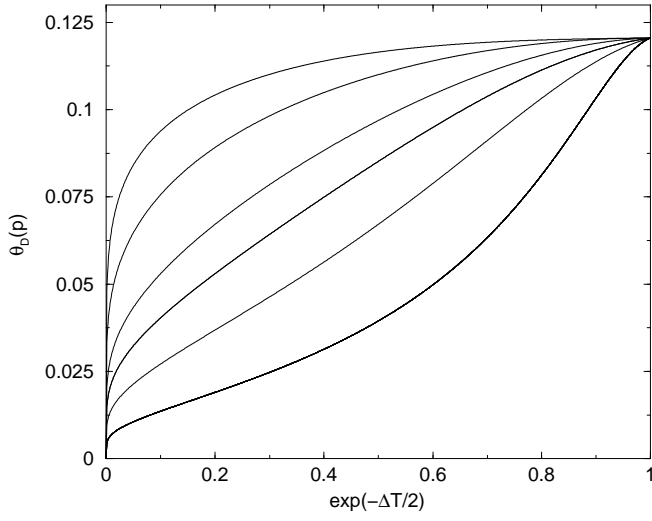


FIG. 17. Plot of  $\theta_D(p)$  against  $\exp(-\Delta T/2)$  for diffusion in 1 dimension with  $p = 0, 1/4, 1/2, 5/8, 3/4$  and  $7/8$  (from the top respectively).  $\theta_D(p)$  has been constrained to give the persistence result at the continuum. The curves are produced from averages of suitable constrained Padés, although in practice the various Padés are indistinguishable.

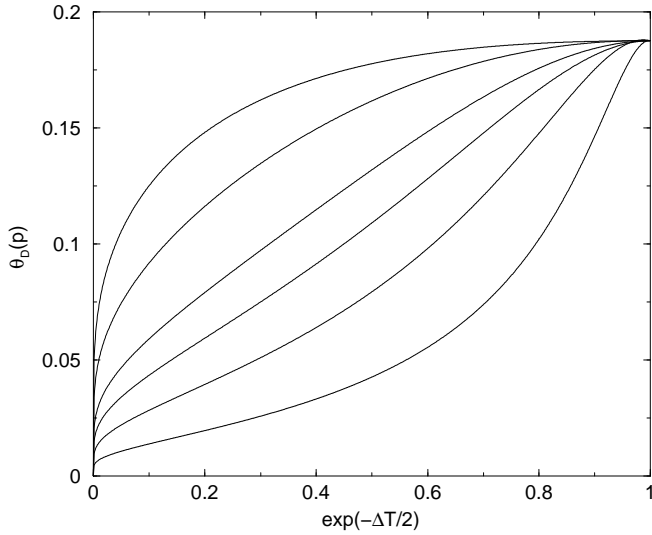


FIG. 18. Plot of  $\theta_D(p)$  against  $\exp(-\Delta T/2)$  for diffusion in 2 dimensions with  $p = 0, 1/4, 1/2, 5/8, 3/4$  and  $7/8$  (from the top respectively).  $\theta_D(p)$  has been constrained to give the persistence result at the continuum. The curves are produced from averages of suitable constrained Padés, although in practice the various Padés are indistinguishable.



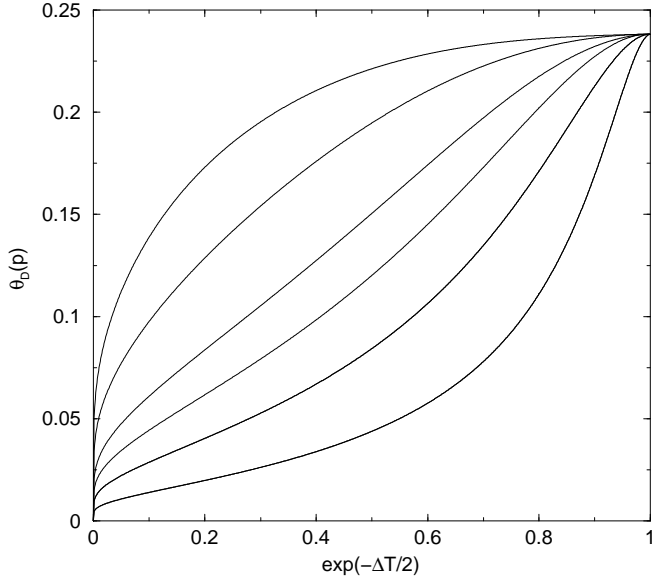


FIG. 19. Plot of  $\theta_D(p)$  against  $\exp(-\Delta T/2)$  for diffusion in 3 dimensions with  $p = 0, 1/4, 1/2, 5/8, 3/4$  and  $7/8$  (from the top respectively).  $\theta_D(p)$  has been constrained to give the persistence result at the continuum. The curves are produced from averages of suitable constrained Padés, although in practice the various Padés are indistinguishable.

A further check is provided by using  $\rho(p)$  to generate the first two cumulants. The results agree term by term to 10th order with the method used to calculate the mean (trivially) and the variance.

We next compare the results obtained by the correlator method to an exactly solvable case, namely the discrete process in Eq. (77) for  $\omega = \pi/4$ . In this case, an exact expression of the exponent  $\theta(p)$  is known [18],

$$\theta(p) = \frac{(1-p)}{2 \tan^{-1} \left( \frac{1-p}{1+p} \right)}. \quad (84)$$

A comparison of this exact result with the one obtained by the correlator method is shown in figure 20.

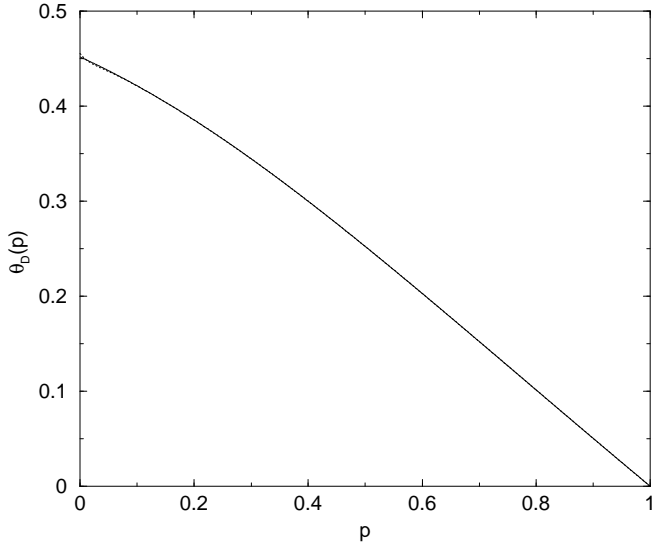


FIG. 20. Plot of  $\theta_D(p)$  against  $p$  for the process  $\psi_i = (\phi_i + \phi_{i-1})/\sqrt{2}$ . The exact (solid line) and raw correlator expansion (dotted line) results are shown, the two curves being indistinguishable except near  $p = 0$

In the last 2 sections we have examined the occupation-time statistics. The occupation time depends only on the signs of  $X(i\Delta T)$  at each  $i$ , that is, it is local. This meant that we merely had to attach additional factors to each local  $X(i\Delta T)$ . In the next sections we will be studying the number of crossings, so we must consider the signs of both  $X(i\Delta T)$  and  $X((i+1)\Delta T)$ . Thus the problem is not local in the sense used above and we cannot just attach additional factors to each  $X(i\Delta T)$ . The solution, as explained in the next section, is to attach additional factors to the lines connecting two  $X$ s in the diagrammatic notation.

## IX. DISTRIBUTION OF CROSSINGS

We now apply the correlator expansion to calculate the distribution of crossings of an arbitrary GSP. We start from the calculation of the persistence. The method is the same up until we assign factors to the diagrams on the lattice. We wish to calculate the probability of  $m$  detected crossings in  $n$  samplings,  $P_{n,m}$ , rather than just the probability of no crossings which was the persistence calculation. To do this, we sum over all the possible ways in which those  $m$  crossings could occur. Furthermore, we note that if we have a line in a diagram connecting two vertices, and  $s$  crossings occur between these two vertices, then the factor  $C(j\Delta T)$  associated with it from the persistence calculation should also have a factor  $(-1)^s$  associated with it. Consider the diagram shown in figure 21.

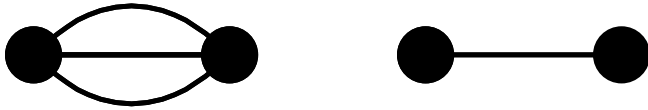


FIG. 21. A 4th order diagram.

Besides the enumerations done for the persistence calculation we must consider the following four cases.

1: No crossings occur on the sites where the diagram is placed. This would occur with probability

$$\frac{(n-m-1)(n-m-2)}{(n-1)(n-2)} \quad (85)$$

and there are no sign changes.

2: There is one crossing between the first and second vertices. This occurs with probability

$$\frac{m(n-m-1)}{(n-1)(n-2)} \quad (86)$$

and there is a factor  $(-1)^3$  associated with it.

3: There is one crossing between the third and fourth vertices. The probability of this occurring is as above and there is a factor  $(-1)$  associated with it.

4: There is one crossing between the first and second vertices and one crossing between the third and fourth vertices. This occurs with probability

$$\frac{m(m-1)}{(n-1)(n-2)} \quad (87)$$

and there is a factor  $(-1)^3(-1)$  associated with it. Hence this diagram has an additional factor

$$\frac{(n-m-1)(n-m-2) - 2m(n-m-1) + m(m-1)}{(n-1)(n-2)} \quad (88)$$

over and above that for the persistence calculation. Furthermore, there is an overall factor

$$\binom{n-1}{m} \quad (89)$$

accounting for all the ways in which the  $m$  crossings can occur on the whole lattice. Note that, although we use the term ‘probability’, when run over the whole lattice (multiplied by the factors  $(n-2)(n-3)/2!$ ) each probability becomes the exact number of ways in which the corresponding event occurs. Thus by introducing these extra rules

when enumerating the diagrams on the lattice we are able to calculate  $P_{n,m}$ , the probability of exactly  $m$  detected crossings occurring in  $n$  samplings. For  $n$  large we expect that, as usual,

$$P_{n,m} \sim \rho_m^n \quad (90)$$

and so we find  $\rho_m$  as

$$\rho_m = \lim_{n \rightarrow \infty} \frac{P_{n+1,m+m/n}}{P_{n,m}}. \quad (91)$$

This has been done, although due to the additional factors it was possible only to go to 10th order due to memory constraints. It has been checked that the result agrees term by term with the normal persistence calculation for  $m = 0$  and with alternating persistence for  $m = n$ . Figures 22, 23, 24, 25, and 26 show  $\rho(r)$  against  $r$  where  $rn = m$  for various values of  $\exp(-\Delta T/2)$  for the random walk, random acceleration, and diffusion in 1-3 dimensions. Notice that, for  $r = \langle r \rangle = 1/2 - (1/\pi) \sin^{-1} C(\Delta T)$ ,  $\rho(r) = 1$ . Close to this point,  $\rho(r)$  approximates to a Gaussian distribution,

$$\rho(r) \propto e^{-\frac{(r - \langle r \rangle)^2}{2(\langle r^2 \rangle - \langle r \rangle^2)}}. \quad (92)$$

where the variance  $\langle r^2 \rangle - \langle r \rangle^2$  agrees term-by-term with the calculation in the following section. Remember that there is a next-to-leading term (pre-exponential factor),  $\sqrt{rtn}$  in  $P_{n,m}$ , as can be seen from considering the  $\Delta T = \infty$  (lowest order) case:

$$P_{n,m} = \frac{1}{2^n} \binom{n-1}{m} \approx \sqrt{\frac{2}{\pi n}} \left( \frac{1}{2} \frac{1}{(1-r)^{1-r} r^r} \right)^n. \quad (93)$$

Note that we are considering the number of detected crossings per sampling (0 or 1). As  $\Delta T \rightarrow 0$  the fraction of (detected) crossings will go to zero. Because of this,  $\theta(r) \rightarrow \infty$  for  $\Delta T \rightarrow 0$  except for the  $r = 0$  case which is just standard persistence. As always,  $0 \leq \rho(r) \leq 1$ , and we choose to plot  $\rho(r)$  rather than  $\theta(r)$ . We have not applied any constraints to the series.

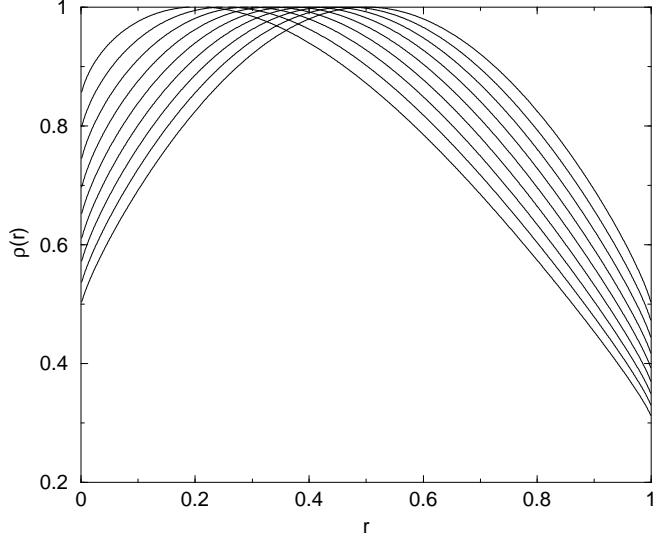


FIG. 22. Plot of  $\rho(r)$  against  $r$  for the random walk with  $\exp(-\Delta T/2) = 0$  to  $8/10$  in steps of  $1/10$  (top right to bottom right respectively). Note that  $\rho(r)$  is 1 at the mean value of  $r$  given by  $\langle r \rangle = 1/2 - \sin^{-1}[C(\Delta T)]/\pi$ . The plots are of the raw series.

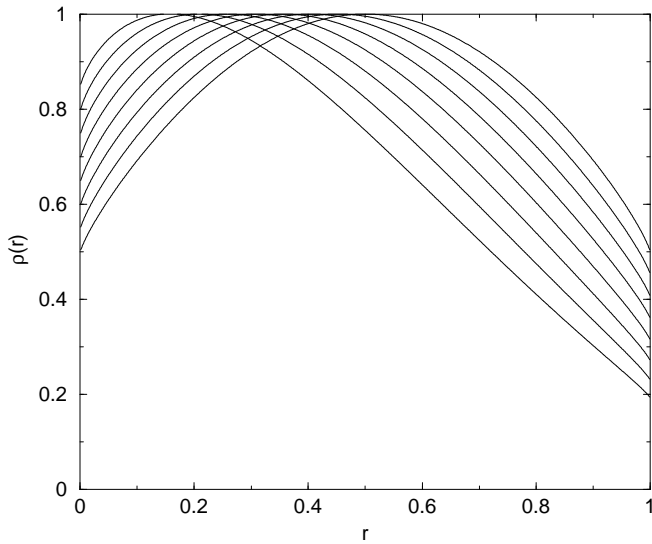


FIG. 23. Plot of  $\rho(r)$  against  $r$  for the random acceleration process with  $\exp(-\Delta T/2) = 0$  to  $7/10$  in steps of  $1/10$  (top right to bottom right respectively). Note that  $\rho(r)$  is 1 at the mean value of  $r$  given by  $\langle r \rangle = 1/2 - \sin^{-1}[C(\Delta T)]/\pi$ . The plots are of the raw series.

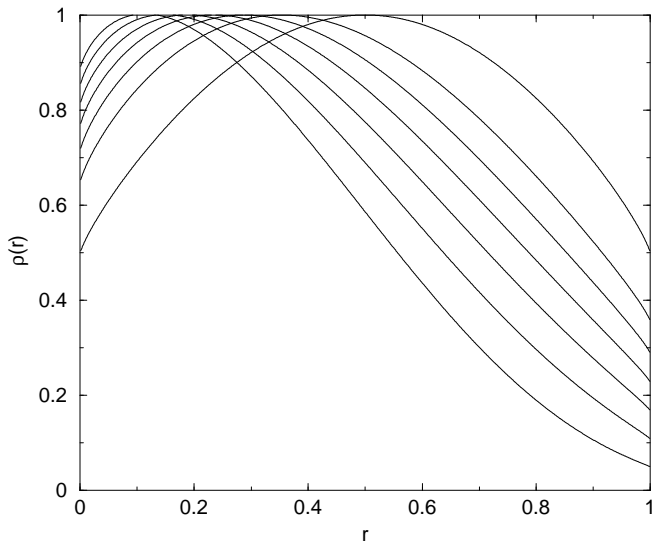


FIG. 24. Plot of  $\rho(r)$  against  $r$  for diffusion in 1 dimension with  $\exp(-\Delta T/2) = 0$  to  $6/10$  in steps of  $1/10$  (top right to bottom right respectively). Note that  $\rho(r)$  is 1 at the mean value of  $r$  given by  $\langle r \rangle = 1/2 - \sin^{-1}[C(\Delta T)]/\pi$ . The plots are of the raw series.

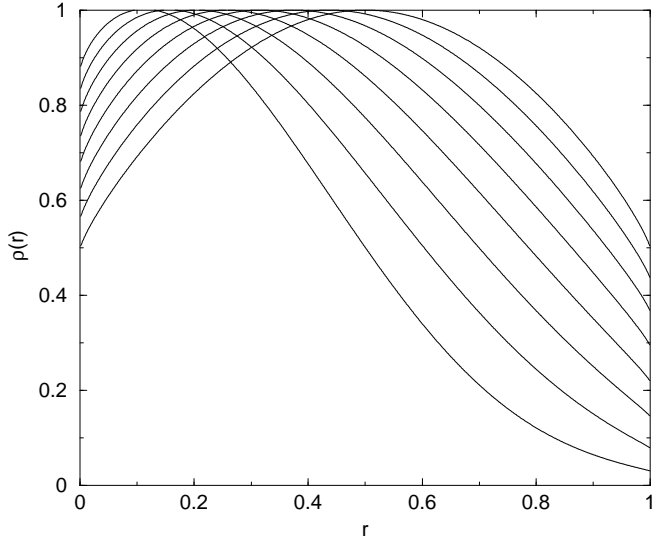


FIG. 25. Plot of  $\rho(r)$  against  $r$  for diffusion in 2 dimensions with  $\exp(-\Delta T/2) = 0$  to  $7/10$  in steps of  $1/10$  (top right to bottom right respectively). Note that  $\rho(r)$  is 1 at the mean value of  $r$  given by  $\langle r \rangle = 1/2 - \sin^{-1}[C(\Delta T)]/\pi$ . The plots are of the raw series.

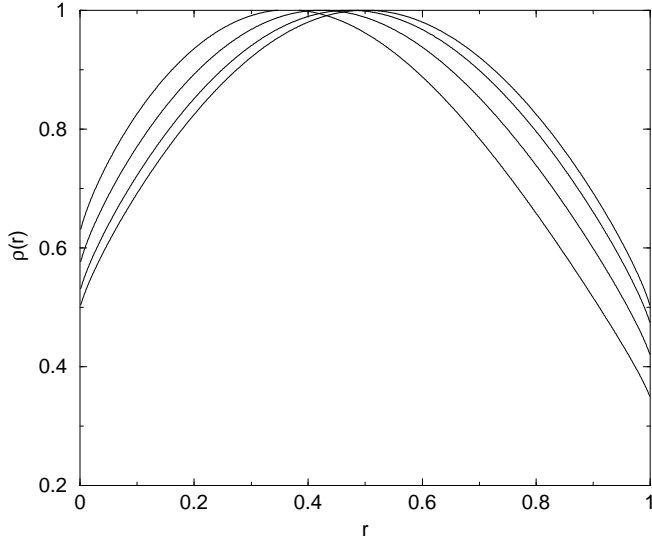


FIG. 26. Plot of  $\rho(r)$  against  $r$  for diffusion in 3 dimensions with  $\exp(-\Delta T/2) = 0$  to  $3/10$  in steps of  $1/10$  (top right to bottom right respectively). Note that  $\rho(r)$  is 1 at the mean value of  $r$  given by  $\langle r \rangle = 1/2 - \sin^{-1}[C(\Delta T)]/\pi$ . The plots are of the raw series.

Recently one of us [5] calculated the distribution of crossings and partial-survival probability of the intrinsically discrete process  $\psi_i$  given by Eq. (77) for the special case  $\omega = \pi/4$ . The correlator of the process is

$$C(i - j) = \delta_{i,j} + \cos \omega \sin \omega (\delta_{i,j-1} + \delta_{i,j+1}). \quad (94)$$

Substituting this into the correlator expansion gives the result shown in figure 27 for comparison with the analytic result. The agreement is good for  $r$  small but for  $r \gtrsim 0.73$  the series has not yet converged by 10th order. This shows up in the way that  $\rho(r)$  changes as the order is increased from 1 to 10. For  $r$  small there is oscillatory convergence whilst for  $r$  large the convergence is monotonic or, for  $r \gtrsim 0.73$ , has not occurred. The fact that convergence does not occur for  $r$  large is presumably because the series is less good for large numbers of crossings. This also occurs, for

example, for the random acceleration problem where the alternating persistence ( $r = 1$ ) result converges more slowly than the standard persistence ( $r = 0$ ) result. That it fails so badly whilst the small  $r$  result is acceptable is surprising. Nevertheless, by checking whether or not the series converges as the order is increased to 10, we can tell whether the result is reliable. For the case  $\omega = \pi/12$ , for which  $C(i-j) = \delta_{i,j} + \frac{1}{4}(\delta_{i,j-1} + \delta_{i,j+1})$ , the series has converged for all  $r$  although there is no analytic result for this case. In fact the case studied is the one for which the correlator takes its largest possible value. Also notice that the  $\rho(1) = 0$  result is due to the requirement that, in order that  $\psi_i$  alternate in sign, the magnitude of  $\phi_i$  must increase every time step. Thus  $P_{n,n}$  decays as  $2^{-n}/n!$ , which is faster than a power of  $n$ , implying  $\rho(1) = 0$ . For other values of the coefficients of  $\phi_i$  and  $\phi_{i-1}$  this is not the case and presumably  $\rho(1)$  is non-zero.

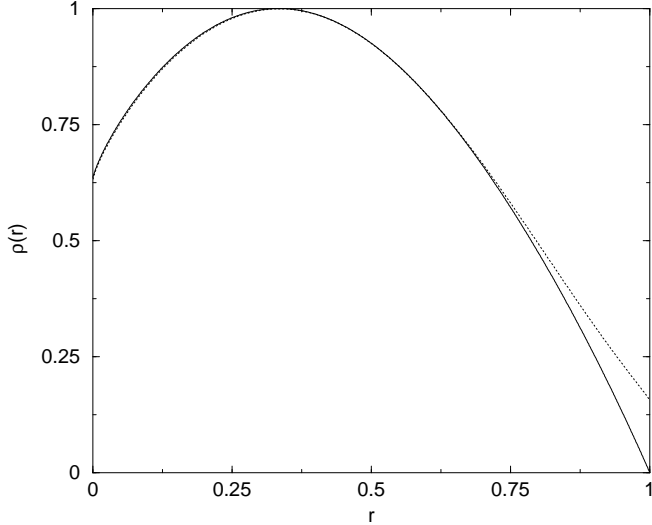


FIG. 27. Plot of  $\rho(r)$  against  $r$  for the process  $\psi_i = (\phi_i + \phi_{i-1})/\sqrt{2}$  where the  $\phi_i$ s are independent identically distributed symmetric random variables. The solid line is the numerical evaluation of the exact result and the dashed line is the result of the correlator expansion. The agreement is good until  $r \sim 0.73$ , and becomes badly wrong as  $r \rightarrow 1$  (see text).

In this section we have calculated the distribution of crossings,  $P_{n,m}$ , to 10th order in the correlator by extending the diagrammatic technique. In the next two sections we derive the standard deviation of the number of crossings and then use  $P_{n,m}$  to calculate  $F_n(p)$ , the partial survival of crossings probability.

## X. THE VARIANCE OF THE NUMBER OF CROSSINGS

The number of detected crossings in  $n$  samplings,  $m$ , is (up to an end effect that is negligible for large  $n$ ),

$$m = rn = \sum_{i=1}^n \frac{1}{2}(1 - \sigma_i \sigma_{i+1}) \quad (95)$$

where  $\sigma_i = \text{sign}[X(i\Delta T)]$ . This gives

$$\langle r \rangle = \frac{1}{2} - \frac{1}{\pi} \sin^{-1}[C(\Delta T)] \quad (96)$$

as derived in [26]. One may further attempt to evaluate the variance of  $m$ ,

$$\sigma^2/n = \left( \langle m^2 \rangle - \langle m \rangle^2 \right) / n = \frac{1}{4n} \sum_{i=1}^n \sum_{j=1}^n \langle \sigma_i \sigma_{i+1} \sigma_j \sigma_{j+1} \rangle - \langle \sigma_i \sigma_{i+1} \rangle \langle \sigma_j \sigma_{j+1} \rangle \quad (97)$$

which involves calculating the connected 4-vertex diagrams in the correlator expansion. The calculation is essentially identical to that of section VI apart from the extra cases of  $i = j$  and  $i = j \pm 1$  and the result to 14th order may be read off. Figures (22 ,23 ,24 ,25 ,26 ,27) show  $\rho(r)$  against  $r$  for various processes and values of  $\Delta T$ . Close to  $r = \langle r \rangle$ ,  $\rho(r)$  is given by

$$\rho(r) \sim \exp \left[ -\frac{1}{2n} \frac{(r - \langle r \rangle)^2}{\langle r^2 \rangle - \langle r \rangle^2} \right] \quad (98)$$

and comparison of  $(r - \langle r \rangle)^2 / [-2n \ln \rho(r)]$  agrees term by term to 14th order in the correlator with the direct calculation of  $\langle r^2 \rangle - \langle r \rangle^2$ , providing a useful cross-check.

The result for  $\langle r^2 \rangle - \langle r \rangle^2$  for the random walk also agrees with that of equation (20) (the matrix method). The variance for various processes is shown in figure 28.

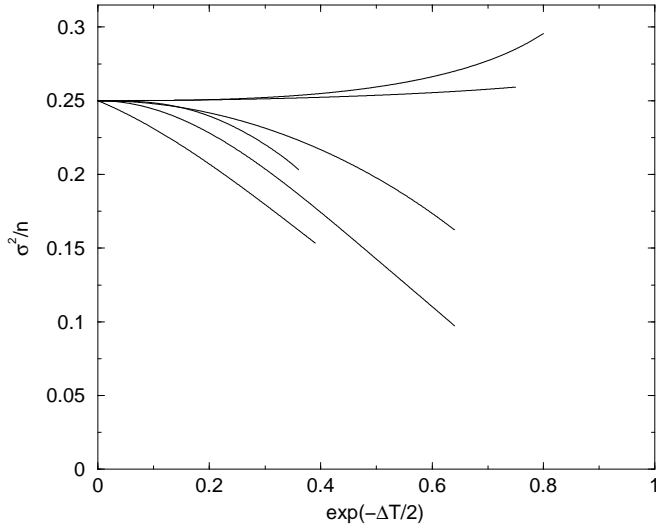


FIG. 28. Plot of  $\sigma^2$  against  $\exp(-\Delta T/2)$ . The curves are, from the top right; the linear growth equation (60), the random walk, random acceleration, and diffusion in 3, 2 and 1 dimensions. The curves are the raw series in powers of  $\exp(-\Delta T/2)$  to 14th order in the correlator and are plotted only as far as their series have converged.

Thus we have found the variance of the number of crossings for an arbitrary process to 14th order in the correlator. This involved calculating the 4-vertex diagrams only, and therefore it is entirely feasible to go to higher orders since the 4-vertex diagrams are relatively simple. Notice also that the variance only contains even orders, as one would expect from the 4-vertex diagrams.

In the following section we complete our calculations by finding the partial-survival probability for an arbitrary GSP, this also being the moment generating function. The results will be shown to agree with those of the current section.

## XI. DISTRIBUTION OF CROSSINGS PARTIAL SURVIVAL

As for the specific case of the random walker (Section V), we may consider the partial-survival probability  $F_n(p)$ , the probability of surviving up to the  $n$ th sampling if each detected crossing is survived with probability  $p$ . As stated in Section V, this is also the generating function for  $P_{n,m}$  and the cumulant generating function [4]:

$$F_n(p) = \sum_{m=0}^n p^m P_{n,m} \quad (99)$$

and

$$\ln F(p) = \sum_{j=1}^{\infty} \frac{(\ln p)^j}{j!} \langle r^j \rangle_c \quad (100)$$

where  $\langle r^j \rangle_c$  is the  $j$ th cumulant. From equation (99) it can be seen that  $F_n(p)$  is a sum of terms containing  $\binom{n}{m} m^s p^m$  where  $s$  is some positive integer. These can be simply evaluated to give an expression for  $F_n(p)$  and hence  $\rho_p$ . As for the occupation partial survival,  $F_n(p) = \rho(p)^n = \exp[-\theta(p)n]$  for all  $n$  even though this is not true for  $P_{n,m}$ .

For rough processes, the continuum partial survival is the same as persistence, since any crossing entails an infinite number of crossings and thus non-survival. For smooth processes however, calculation of  $\rho(p)$  and hence that of  $\theta(p) = -\ln[\rho(p)]$  is non-trivial. For the random acceleration problem the exact result is [32],

$$\theta(p) = \frac{1}{4} \left( 1 - \frac{6}{\pi} \sin^{-1} \frac{p}{2} \right). \quad (101)$$

Whilst for the intrinsically discrete process (equation (77)) it is [5],

$$\theta(p) = \ln \left( \frac{\sin^{-1} \sqrt{1-p^2}}{\sqrt{1-p^2}} \right). \quad (102)$$

Figure 29 shows this result and the raw series result for comparison.

For general processes we apply the constraint to the series that  $\rho(p)|_{\Delta T=0} = 1$ . For sufficiently smooth processes, as before, the first correction to  $\theta(p)$  near  $\Delta T = 0$  will be of order  $\Delta T^2$ . We apply this additional constraint to the appropriate processes and the corresponding continuum results are shown in figures 30, 31.

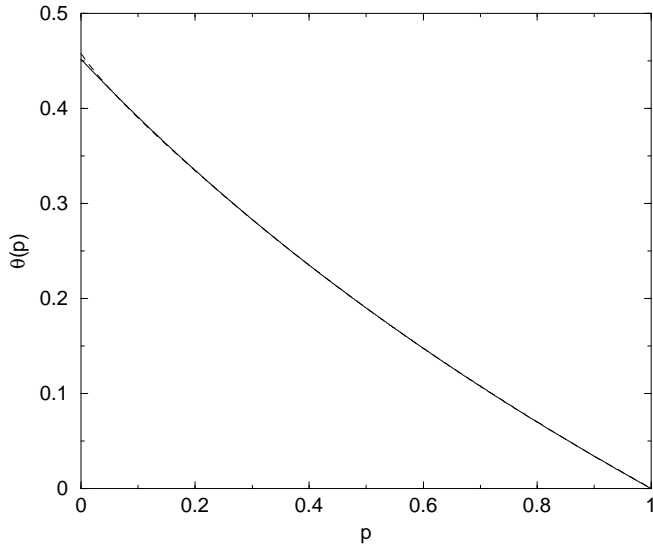


FIG. 29. Plot of  $\theta(p)$  against  $p$  for the process  $\psi_i = (\phi_i + \phi_{i-1})/\sqrt{2}$ . The solid line is the exact result and the dashed line is the result of the correlator expansion. They differ by a maximum of 0.00576 (at  $p = 0$ ).



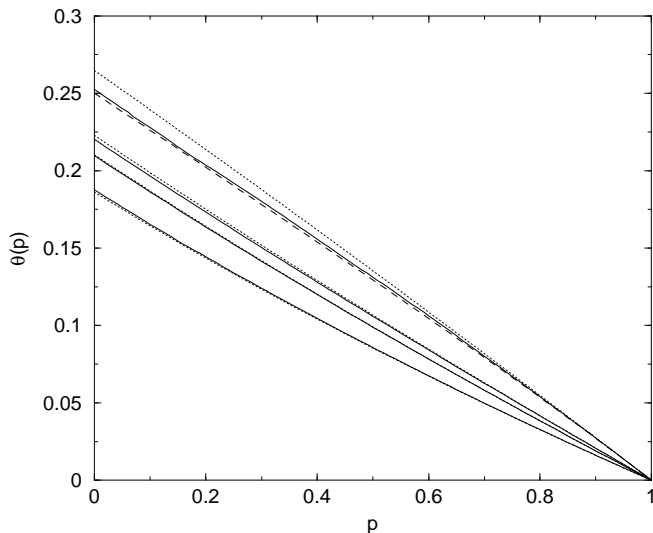


FIG. 30. Plot of  $\theta(p)$  against  $p$  for (top to bottom) the  $d^n x/dt^n = \eta(t)$  process with  $n = 2$  (random acceleration),  $n = 3$ ,  $n = 4$ , and  $n \rightarrow \infty$  (equivalent to diffusion in 2 dimensions). For  $n = 2$  (top curves) the exact result (101) is shown (dashed line) along with the IIA (dotted) and the Padé with 1 constraint (solid line). For the other cases, the IIA (dotted) and Padé with 2 constraints (solid line) are shown. The correlator results are an average of suitable Padés of order 10 to 7. Note that the IIA is rather inaccurate for the random acceleration, but improves as  $n$  increases.

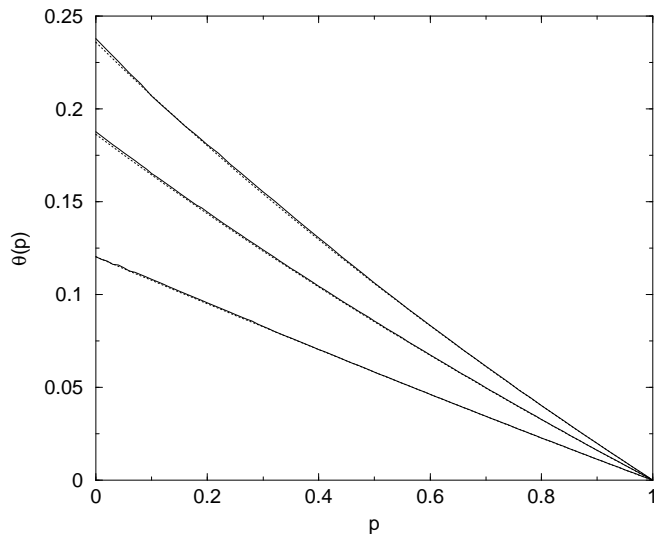


FIG. 31. Plot of  $\theta(p)$  against  $p$  for diffusion in 1, 2 and 3 dimensions (bottom to top). The IIA results (dotted) and the correlator results (solid lines) are plotted. The correlator results are an average of suitable Padés of order 10 to 7 for 1 and 2 dimensions and 6 to 5 for 3 dimensions.

The results from the matrix method partial survival for the random walk and random acceleration agree with those of the correlator expansion term by term to within the numerical error of the matrix method. Also, using  $F_n(p)$  as a generating function, we find that the first two cumulants agree term by term to 10th order with the results of section X. We are also able to calculate higher cumulants. We have also used the method of steepest descents to calculate  $\rho(r)$  from  $\rho(p)$  as a further cross-check.

This evaluation of the crossing partial survival completes our calculations.

## XII. CONCLUSION

In this paper we have used the correlator expansion to calculate several properties of an arbitrary discrete or discretely sampled Gaussian Stationary Process. The expansion in powers of the correlator works well when the variables are relatively weakly correlated. For stronger correlations the series expansion does not converge. We are however able, for the case of an underlying continuous and sufficiently smooth process, to extrapolate our results all the way to the continuum by using the Padé Approximant with two constraints. Thus even in the continuum we have been able to calculate the persistence exponents, the occupation-time exponents and the partial survival of crossings exponents to high precision. These results compare well with those of the Independent Interval Approximation, the other general method. In most cases they are more accurate, however, and they also give an estimate of the error of the result which the IIA does not. Furthermore, by calculating higher orders the results may be improved. We believe we have demonstrated convincingly that the correlator expansion is the method of choice for calculating persistence properties of Gaussian stationary processes.

## XIII. ACKNOWLEDGEMENTS

GE thanks Andrew Stephenson for useful discussions, and EPSRC(UK) for a Research Studentship.

- 
- [1] S.O. Rice, *Bell Syst. Tech. J.* **23**, 282 (1944); **24**, 46 (1945).
  - [2] J.S. Bendat, *Principles and Applications of Random Noise Theory* (Wiley, New York, 1958).
  - [3] I.F. Blake and W.C. Lindsey, Level crossing problems for random processes, *IEEE Trans. Inform. Theory*, Vol. IT-19, pp 295-315 (1973).
  - [4] S.N. Majumdar and A.J. Bray, *Phys. Rev. Lett.* **81**, 2626 (1998).
  - [5] S.N. Majumdar, *Phys. Rev. E* **65**, 035104 (2002).
  - [6] P. Lévy, *Composito Mathematica* **7**, 238 (1939).
  - [7] M. Kac, *Trans. Am. Math. Soc.* **65**, 1 (1949); D.A. Darling and M. Kac, *Tran. Am. Math. Soc.* **84**, 444 (1957); For a recent review of the occupation time in the mathematics literature see S. Watanabe, *Proc. Symp. Pure Math.* **57**, 157 (1995).
  - [8] J.Lamperti, *Trans. Am. Math. Soc.* **88**, 380 (1958).
  - [9] I. Dornic, and C. Godrèche, *J. Phys. A* **31**, 5413 (1998).
  - [10] T.J. Newman, and Z. Toroczkai, *Phys. Rev. E* **58**, R2685 (1998).
  - [11] A. Dhar and S.N. Majumdar, *PRE* **59**, 6413 (1999).
  - [12] I. Dornic, A. Lamaitre, A. Baldassari, and H. Cahté, *J. Phys. A: Math. Gen.* **33**, 7499 (2000); G. De Smedt, C. Godrèche, and J.M. Luck, *J. Phys. A: Math. Gen.* **34**, 1247 (2001).
  - [13] T.J. Newman and W. Loinaz, *Phys. Rev. Lett.* **86**, 2712 (2001).
  - [14] G.H. Weiss and P.P. Calabrese, *Physica-A (Amsterdam)*, **234**, 443 (1996).
  - [15] Z. Toroczkai, T.J. Newman, and S. Das Sarma, *Phys. Rev. E* **60**, R1115 (1999).
  - [16] S. N. Majumdar and A. J. Bray, *Phys. Rev. E* **65**, 051112 (2002).
  - [17] S.N. Majumdar and A. Comtet, *Phys. Rev. Lett.* **89**, 060601 (2002).
  - [18] S.N. Majumdar and D.S. Dean, *Phys. Rev. E* **66**, 041102 (2002).
  - [19] For a recent review on persistence, see S.N. Majumdar, *Curr. Sci.* **77**, 370 (1999), also available on cond-mat/9907407.
  - [20] S.N. Majumdar, C. Sire, A.J. Bray, and S.J. Cornell, *Phys. Rev. Lett.* **77**, 2867 (1996).
  - [21] B. Derrida, V. Hakim, and R. Zeitak, *Phys. Rev. Lett.* **77**, 2871 (1996).
  - [22] R. Zeitak, *Phys. Rev. E* **56**, 2560 (1997).
  - [23] S.N. Majumdar, A.J. Bray and G.C.M.A. Ehrhardt, *Phys. Rev. E* **64**, 015101(R) (2001).
  - [24] G.C.M.A. Ehrhardt, A.J. Bray and S.N. Majumdar, *Phys. Rev. E* **65**, 041102 (2002).
  - [25] G.C.M.A. Ehrhardt and A.J. Bray, *Phys. Rev. Lett.* **88**, 070601 (2002); the 14th correlator expansion for a general GSP is given in cond-mat/0109526.
  - [26] A.M. Barbé, *IEEE Trans. Inform. Theory*. vol. IT-22, pp.96-102 (1976).
  - [27] Gaunt, D.S. and Guttman, A.J. (1974). In *Phase Transitions and Critical Phenomena*, Vol. 3 (eds C. Domb and M.S. Green), pp.202-3.

- [28] J. Krug et al., Phys. Rev. E **56** 2702 (1997).
- [29] B.B. Mandelbrot and J.W. van Ness, SIAM Review **10**, 422 (1968).
- [30] S.N. Majumdar and D. Dhar, Phys. Rev. E **64**, 046123 (2001).
- [31] B. Derrida and E. Gardner, J. Phys. (Paris) **47**, 959 (1986).
- [32] T. W. Burkhardt, J. Phys. A **33**, L429 (2000).